HHS Public Access

Author manuscript

Dev Cell. Author manuscript; available in PMC 2018 May 22.

Published in final edited form as:

Dev Cell. 2017 May 22; 41(4): 349–365.e3. doi:10.1016/j.devcel.2017.04.022.

Repression of interstitial identity in nephron progenitor cells by *Pax2* establishes the nephron-interstitium boundary throughout kidney development

Natalie Naiman[1], **Kaoru Fujioka**[1], **Mari Fujino**[2], **M. Todd Valerius**[1], **S. Steven Potter**[4], **Andrew P. McMahon**[5], and **Akio Kobayashi**[1,2,*]

[1]Department of Medicine, Brigham and Women's Hospital, Harvard Medical School, 77 Avenue Louis Pasteur, Boston, MA 02115

[2]Department of Medicine, Institute for Stem Cell and Regenerative Medicine, University of Washington, 750 Republican Street, Seattle, WA 98109

[4]Cincinnati Children's Medical Center, Division of Developmental Biology, 3333 Burnet Ave., Cincinnati, OH, 45229

[5]Department of Stem Cell Biology and Regenerative Medicine, Eli and Edythe Broad-CIRM Center for Regenerative Medicine and Stem Cell Research, W.M. Keck School of Medicine of the University of Southern California, 1425 San Pablo Street, Los Angeles, CA 90033, USA

SUMMARY

The kidney contains the functional units, the nephrons, surrounded by the renal interstitium. Previously, we discovered that, once *Six2*-expressing nephron progenitor cells and *Foxd1*-expressing renal interstitial progenitor cells form at the onset of kidney development, descendant cells from these populations contribute exclusively to the main body of nephrons and renal interstitial tissues, respectively, indicating a lineage boundary between the nephron and renal interstitial compartments. Currently, it is unclear how lineages are regulated during kidney organogenesis. We demonstrate that nephron progenitor cells lacking *Pax2* fail to differentiate into nephron cells, but can switch fates into renal interstitium-like cell types. These data suggest that *Pax2* function maintains nephron progenitor cells by repressing a renal interstitial cell program. Thus, the lineage boundary between the nephron and renal interstitial compartments is maintained by the *Pax2* activity in nephron progenitor cells during kidney organogenesis.

eTOC BLURB

*Lead Contact (akiok@uw.edu, Phone +1-206-616-6244).

AUTHOR CONTRIBUTIONS

Conceptualization, A.K.; Methodology, S.S.P. and A.K.; Investigation, N.N., K.F., M.F., S.S.P. and A.K.; Resources, M.T.V. and A.P.M.; Writing – Original Draft, A.K.; Writing – Review & Editing, M.T.V., S.S.P., A.P.M. and A.K.; Funding Acquisition, A.P.M. and A.K.

The lineage boundary exists between the nephron and interstitial compartments in the kidney. It is currently unclear how lineage boundaries are formed during kidney development. Naiman et al. show that repression of interstitial fates in nephron progenitor cells by *Pax2* establishes the nephron-interstitium boundary throughout kidney organogenesis.

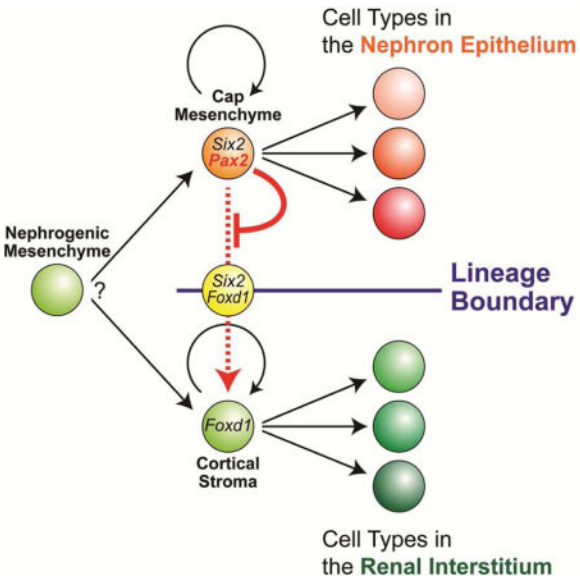

Keywords

kidney; nephron; progenitor; cell fate; PAX2

INTRODUCTION

The kidney is a vital organ removing metabolic waste products from the blood and maintaining water/ion balance for the body. The functional unit of the kidney, the nephron, is surrounded by the renal interstitial tissues (Little et al., 2007). The human and mouse kidney contain about one million and 13,000 nephrons, respectively (Bertram et al., 2014; Cebrian et al., 2004). Reduced nephron endowment is associated with the future development of hypertension and potentially chronic kidney diseases (CKD), leading to end stage renal disease (ESRD) (Luyckx and Brenner, 2015), a significant, growing economic health burden in the USA. In mammals, nephrons are generated only during kidney development: no *de novo* nephron-forming ability resides within the adult kidney (Hartman et al., 2007; Romagnani et al., 2013). An understanding of the regulatory mechanisms governing nephron formation is critical not only to clarify how the functional kidney forms a full complement of nephrons, but also to develop therapeutic strategies to increase nephron endowment where premature birth, malnutrition or other pathological conditions have reduced nephron number (Hendry et al., 2013; Taguchi et al., 2014; Takasato et al., 2015).

During mammalian embryogenesis, the urogenital system including the kidney arises from the intermediate mesoderm of the developing embryo (Saxen, 1987; Stewart and Bouchard, 2014). Formation of the kidney is initiated by reciprocal interactions of two adjacent tissues,

the ureteric bud and metanephric mesenchyme, from 10.5 days post coitus (dpc) of mouse development (Costantini and Kopan, 2010; Little and McMahon, 2012). As the ureteric bud grows into the metanephric mesenchyme, the *Six2*-expressing (*Six2*$^{+}$) condensed cap mesenchyme becomes surrounded by the *Foxd1*$^{+}$ cortical stroma (the renal capsule and nephrogenic interstitium) in the mesenchyme (Hatini et al., 1996; Levinson and Mendelsohn, 2003). While the ureteric tip grows and branches repetitively to form the collecting duct system of the kidney (Costantini, 2012), cap mesenchyme cells remain condensed around each branch tip. A subset of cap mesenchyme cells commits to a nephron differentiation program through the establishment of a pretubular aggregate (Stark et al., 1994). The pretubular aggregate subsequently undergoes epithelial formation to a renal vesicle, which further differentiates into the comma- and S-shaped bodies, and eventually the main body of the nephron (the nephron epithelium): the visceral (podocyte) and parietal epithelium of the glomerulus, proximal tubule, loop of Henle and distal tubule (Boyle et al., 2007; Kobayashi et al., 2008).

The mature nephron is surrounded by the renal cortical and medullary interstitium (Alcorn et al., 1999; Lemley and Kriz, 1991). Podocytes of the glomerulus surround the glomerular capillary system, including the mesangium and endothelium (Boyle et al., 2014; Lin et al., 2014; Quaggin and Kreidberg, 2008). Outside of the glomerulus, the vasculature is supported by perivascular cells (pericytes) (Herzlinger and Hurtado, 2014; Sequeira Lopez and Gomez, 2011). The renal capsule, the nephrogenic, renal cortical and medullary interstitium, the mesangium and the peri-vasculature compose the renal interstitium (Little et al., 2007).

Our fate map analysis previously revealed that the *Six2*$^{+}$ cap mesenchyme is a multipotent self-renewing progenitor population for the nephron epithelium (Kobayashi et al., 2008). Furthermore, we identified that the *Foxd1*$^{+}$ cortical stroma is another multipotent self-renewing progenitor population for the renal interstitium (Kobayashi et al., 2014). The *Six2*$^{+}$ cap mesenchyme and *Foxd1*$^{+}$ cortical stroma exclusively contribute to nephron epithelial and renal interstitial tissues, respectively, although there are minor cell fate changes of contribution of *Foxd1*+ cells to the nephron lineage (Brunskill et al., 2014; Kobayashi et al., 2014). Mature nephron and renal interstitial compartments are also maintained during kidney fibrosis and nephron regeneration in adults with little (LeBleu et al., 2013; Pippin et al., 2013) or no evidence (Humphreys et al., 2008; Humphreys et al., 2010) of cell type switching between the lineage-restricted cellular compartments. Thus, once nephron and renal interstitial progenitor cells are specified at the onset of kidney development, their descendants maintain distinct fates segregated by a lineage boundary in normal, diseased and regenerating kidneys. However, it is currently unclear how such lineage boundaries are regulated during kidney development.

The paired-domain transcriptional regulator *Pax2* is expressed in multiple urogenital tissues, including the nephric (Wolffian) duct, cap mesenchyme, and differentiating nephron and collecting duct system of the developing kidney (Dressler et al., 1990). Global inactivation of *Pax2* in the mouse results in agenesis of the kidney, ureter and male reproductive tract due to degenerating nephric ducts prior to the initiation of (metanephric) kidney development (Ranghini and Dressler, 2015; Torres et al., 1995), while combined removal of *Pax2* and

Pax8 leads to a complete absence of nephric duct development, also resulting in kidney agenesis (Bouchard et al., 2002). Although *Pax2* has been widely recognized as a key regulatory factor in kidney development (Brophy et al., 2001; Rothenpieler and Dressler, 1993), because of the kidney agenesis in *Pax2*-null mouse mutants, *Pax2* function in distinct tissues within the developing kidney has not been defined *in vivo*.

Our data herein suggest that *Pax2* function in the cap mesenchyme is required to maintain nephron progenitor cells mainly by repressing transdifferentiation into renal interstitium-like cell fates. Thus, *Pax2* activity in nephron progenitor cells maintains the lineage boundary between the nephron and renal interstitial compartments during mammalian kidney organogenesis.

RESULTS

PAX2 is co-expressed with SIX2 in the cap mesenchyme, but not with FOXD1 in the renal cortical stroma during kidney organogenesis

PAX2 is expressed in the mesenchyme surrounding the PAX2-expressing ($PAX2^+$) ureteric epithelium and differentiated derivatives of $SIX2^+$ progenitors in the developing kidney (Dressler and Douglass, 1992). First, we closely examined PAX2 expression in progenitor populations during early stages of kidney organogenesis. Around the posterior nephric duct at 10.5 dpc, PAX2 expression was detected in $SIX2^+$ metanephric mesenchyme cells and $SIX2^-$ cells in the nephric duct and ureteric bud. At this stage, FOXD1 expression was largely absent except for a few mesenchymal cells starting to express FOXD1 at very low levels outside of the $SIX2^+$ metanephric mesenchyme (Fig 1A–D). One day later at 11.5 dpc, when the ureteric bud grows and branches once to form two ureteric tips, PAX2 expression was observed in $SIX2^+$ cap mesenchyme cells and $SIX2^-$ ureteric tip cells, but not in scattered $FOXD1^+$ renal cortical stroma cells around $SIX2^+$ cells (Fig 1E–H). At 15.5 dpc, PAX2 is expressed in $SIX2^+$ cap mesenchyme cells and a subset of differentiating nephron cells, but not surrounding $FOXD1^+$ renal cortical stroma cells (Fig 1I–L) as previously shown (Hatini et al., 1996). We did not detect $SIX2^+$ $FOXD1^+$ double positive cells using confocal immunofluorescence throughout kidney development except for very rare cells (data not shown, see below). Although a recent single cell RNA-seq analysis identified rare cells expressing both *Six2* and *Foxd1* mRNA, the *Foxd1* mRNA was partially degraded in these $Six2^+$ $Foxd1^+$ cells (Brunskill et al., 2014), which indicates that our observations are consistent.

Generation of a conditional *Pax2*-null allele in the mouse

Because *Pax2* is required to maintain the nephric (Wolffian) duct, there is no induction of kidney (metanephros) development in *Pax2*-null mutant mice (Torres et al., 1995). To examine *Pax2* function at later stages in the nephron progenitor population, we first generated a Cre/*lox*P-dependent conditional *Pax2*-null mouse allele where a conditional removal of exon 2 results in a frame-shift mutation with a premature termination, producing a transcript encoding only the first 14 amino acids of a normal 393 amino acid PAX2 protein (Dressler, 2011) (Fig S1A,B). This predicted null allele is designated as $Pax2^{del}$; the conditional allele (with selection cassette removed) is referred to as $Pax2^{flox}$ (Fig S1A).

To validate the *Pax2*^{flox} allele, *Pax2*$^{flox/+}$ mice were mated with an epiblast-specific *Sox2-Cre* mice (Hayashi et al., 2002) to generate *Pax2* deleted (*Pax2*$^{del/+}$) mice (Fig S1C). While *Pax2*$^{flox/flox}$ embryos were phenotypically normal at 18.5 dpc (Fig S1D), *Pax2*$^{del/del}$ embryos showed identical abnormalities to those of *Pax2*-null (*Pax2*$^{-/-}$) mutant mice (Torres et al., 1995), including a complete absence of the kidney, ureter and reproductive tracts (Fig S1E), which validates the conditional *Pax2*-null mouse allele.

Inactivation of *Pax2* in the cap mesenchyme of the developing kidney

To investigate *Pax2* function in the cap mesenchyme, we inactivated *Pax2* using the *Six2-eGFPCre* BAC transgenic (*Six2-eGFPCre*$^{tg/+}$) mice (Kobayashi et al., 2008). To confirm *Pax2* inactivation by the *Six2-eGFPCre* transgene, we examined PAX2 expression in *Pax2* cap mesenchyme-specific knock-out mutant (*Pax2* CM KO) kidneys from *Six2-eGFPCre*$^{tg/+}$; *Pax2*$^{flox/del}$ embryos using an anti-mouse PAX2 antibody against amino acids 188–385, which are absent from the translated product of the *Pax2*^{del} allele. In kidneys from *Six2-eGFPCre*$^{tg/+}$; *Pax2*$^{flox/+}$ control littermates at 12.5 dpc, PAX2 expression was detected in the cap mesenchyme, differentiating nephrons and cytokeratin^{+} (KRT^{+}) developing collecting duct system including the ureteric tip (Fig 1M), while *Six2*-GFP expression was detected strongly in the cap mesenchyme and weakly in the immature nephron precursors (Fig 1O). In *Pax2* CM mutant kidneys at the same stage, PAX2 expression was greatly reduced in the *Six2*-GFP^{+} cap mesenchyme cells (Fig 1N,P). PAX2 expression was observed in some *Six2*-GFP negative (*Six2*-GFP^{-}) cells in the cap mesenchyme and differentiating nephrons (yellow and white arrows in Fig 1N,P, respectively), most likely due to delayed onset of the mosaic *Six2-eGFPCre* transgene expression (Kobayashi et al., 2008; Park et al., 2007). At 13.5 dpc, PAX2 expression was not detected in the cap mesenchyme of *Pax2* CM mutant kidneys, except for a few rare cells (Fig 1Q–T). These data suggest that *Pax2* was specifically inactivated in the majority of cap mesenchyme cells during early stages of kidney organogenesis.

Pax2 function is required for development of the cap mesenchyme

To determine the effect of *Pax2* inactivation in the cap mesenchyme, we examined phenotypes of the urogenital system. We found that *Pax2* CM mutants die within 24 hours of birth, around 19 dpc. Unlike *Pax2*-null (*Pax2*$^{-/-}$) mutant neonates at birth (Torres et al., 1995), *Pax2* CM mutant mice showed a vestigial kidney structure connected to a ureter and reproductive tracts including the epididymis and vas deferens in males (Fig 2A–D, S1E). Histological analysis revealed that the *Pax2* CM mutant kidneys lacked the cap mesenchyme and all but a few nephrons that were PAX2^{+} (Fig 2C–F and data not shown), reflecting early escape from Cre recombination probably due to the delayed onset of the *Six2-eGFPCre* transgene. Thus, *Pax2* function is required for development of the cap mesenchyme in the developing kidney.

In control kidneys at 18.5 dpc, PAX2 was expressed in the cap mesenchyme, differentiating nephron epithelium, KRT^{+} ureteric tip and KRT^{high} collecting duct, but not in the PDGFRB^{+} renal interstitium (Fig 2G). In *Pax2* CM mutant kidneys at this stage, PAX2 expression was observed only in the KRT^{high} collecting duct (white arrow in Fig 2H). Most cells outside of the KRT^{high} collecting duct were PDGFRB^{+} renal interstitial cells (Fig 2H). While FOXD1

expression was normally detected in the cortical region, SIX2 expression was absent (Fig 2I,J, S2A–B and data not shown), except for in rare PAX2$^+$ cells adjacent to the rare ureteric tip in *Pax2* CM mutants (yellow arrow in Fig 2J and data not shown). All the other cap mesenchyme markers examined, including CITED1 and N-cadherin (CDH2), were not detected (see below), suggesting that the cap mesenchyme may fail to undergo normal development in *Pax2* CM mutants.

We also examined nephron differentiation in *Pax2* CM mutant kidneys. In control kidneys at 18.5 dpc, a KRT$^{-\text{ or low}}$ Laminin$^+$ (LAM$^+$) E-cadherin$^+$ (CDH1$^+$) differentiating nephron epithelium was observed together with a KRT$^+$ LAM$^+$ CDH1$^+$ ureteric tip and KRT^{high} LAM$^+$ CDH1$^+$ collecting duct (Fig 2K). In *Pax2* CM mutant kidneys, no KRT$^{-\text{ or low}}$ LAM$^+$ CDH1$^+$ nephron epithelium was detected, except for a few nephrons that escaped Cre recombination (Fig 2L). Segmental nephron organization in control kidneys was evident by examining Podocalyxin (PODXL) and Podocin (NPHS2) (visceral epithelium, podocytes), *Lotus Tetragonolobus* Lectin (LTL) (proximal tubule), Uromodulin (UMOD; also known as Tamm-Horsfall Glycoprotein) (loop of Henle) and SLC12A3 (also known as NCC) (distal tubule) (Fig 2M,M′ and data not shown). In contrast, none of the nephron segment markers were detected in *Pax2* CM mutant kidneys (Fig 2N,N′). Low PODXL expression was observed in the endothelium (Fig 2M–N′). These molecular marker data confirm that *Pax2* inactivation in the cap mesenchyme results in loss of the nephron epithelium.

In the interstitium of control kidneys at 18.5 dpc, Tenascin C (TNC) expression was observed in the renal capsule, nephrogenic/renal cortical interstitium and innermost medullary interstitium adjacent to the pelvic urothelial lining, Vimentin (VIM) expression in the renal cortical and medullary interstitium, and α-smooth muscle actin (ACTA2) expression in the outer medullary interstitium (Fig 2O–O″). In the *Pax2* CM mutants, TNC and VIM expression domains were observed along a cortico-medullary axis of the kidney, but strong ACTA2 expression was not observed (Fig 2O′,P′). These data suggest that renal interstitium differentiation along the cortico-medullary axis of the kidney was largely normal even without nephron formation in *Pax2* CM mutants, although there was likely some secondary effect that results in a failure of development of ACTA2$^+$ outer renal medullary interstitial cells.

In *Pax2* CM mutants, focal dense tissues were observed around the rare ureteric tips on the surface of the kidney (yellow arrowheads in Fig 2D,F). Molecular marker analysis at 18.5 dpc showed a few *Six2*-GFP$^-$ SIX2$^+$ PAX2$^+$ cells surrounding rare ureteric tips (Fig S2A–B″″), indicating that the dense tissues contain some cap mesenchyme cells that escaped *Pax2* inactivation probably due to the mosaic *Six2- eGFPCre* expression. LIV2 was detected in the connective tissue surrounding the kidney and adrenal gland, and renal capsule in control kidneys (Fig S2E) (Kobayashi et al., 2014). Molecular marker analysis revealed that the dense tissues are a heterogeneous population containing LIV2$^+$ FOXD1$^-$ PDGFRB$^-$ CDH2$^+$ TNC$^-$ VIM$^+$ connective tissue cells and LIV2$^+$ FOXD1$^+$ PDGFRB^{low} CDH2^{low} TNC$^+$ VIM$^-$ renal capsule cells (Fig S2C–L). These data suggest that the dense tissues formed by expansion of both the connective tissue and renal capsule around the rare ureteric tips surrounded by some PAX2$^+$ cap mesenchyme cells.

Pax2 function is required to maintain the cap mesenchyme

At the T-shaped ureteric stage at 11.5 dpc, high *Six2*-GFP expression was observed in the cap mesenchyme surrounding the ureteric tips in both control and *Pax2* CM mutant kidneys, indicating that the cap mesenchyme is formed in both control and mutant kidneys initially (Fig 2Q–R′). As the ureteric tips continue to grow and branch, cap mesenchyme cells remained tightly condensed around the ureteric tips, surrounded by the renal interstitial progenitor cells in control kidneys (Fig 2S,U,W,Y,Y′). The developing nephrons, including the pretubular aggregate, renal vesicles, and comma- and S-shaped bodies, were observed (Fig 2U,Y′ and data not shown). In contrast, in *Pax2* CM mutant kidneys at 12.5 dpc, a tightly packed cap mesenchyme was less evident (Fig 2T,V). In *Pax2* CM mutant kidneys at 13.5 dpc, the cap mesenchyme and differentiating nephrons were not observed and the ureteric tip was directly surrounded by interstitium-like cells (Fig 2X,Z,Z′).

These results show that in *Pax2* CM mutants, the early cap mesenchyme properly drives cap mesenchyme-dependent ureteric bud branching. Nevertheless, *Pax2* function is essential to maintain the cap mesenchyme nephron progenitor pool after its initial specification from 11.5 dpc. Whether *Pax2* plays an earlier role in specifying this population at 10.0–10.5 dpc cannot be addressed in this genetic model due to the delayed onset of expression of the *Six2-eGFPCre* transgene.

Pax2 function maintains the cell status of cap mesenchyme cells

Next, we examined how *Pax2* function maintains cap mesenchyme cells. One possibility is that *Pax2* is required for survival of cap mesenchyme cells and loss of *Pax2* results in death of cap mesenchyme cells. Another possibility is that *Pax2* function maintains the cellular identity of cap mesenchyme cells and *Pax2*-deficient cap mesenchyme cells undergo a cell fate switch.

To address these potential outcomes, we visualized the fate of cap mesenchyme cells by incorporating a *Rosa26-lacZ* Cre reporter allele (Soriano, 1999) into *Pax2* CM mutants. In *Six2-eGFPCre*$^{tg/+}$; *Pax2*$^{flox/del}$; *R26R*$^{lacZ/+}$ mice, all *Pax2*-deficient descendant cells derived from the cap mesenchyme express β-gal. *Six2-eGFPCre*$^{tg/+}$; *Pax2*$^{flox/+}$; *R26R*$^{lacZ/+}$ littermates were used for controls. In control kidneys, we observed the contribution of β-gal^{+} cells into differentiating cap mesenchyme-derivatives but not to renal interstitial progenitors or their derivatives as expected (Fig 3A,C,E,G). However, in *Pax2* CM mutant kidneys at 13.5 dpc (Fig 3B,D), some β-gal^{+} cells showed a round cell shape around the ureteric tip, while other β-gal^{+} cells became dispersed away from the ureteric tip within the renal interstitium (yellow arrows and arrowheads in Fig 3D, respectively). β-gal^{+} cells persisted within the renal interstitium of the rudimentary mutant kidney at 18.5 dpc (yellow arrowheads in Fig 3F,H), suggesting that *Pax2*-deficient nephron progenitor cells may adopt ectopic renal interstitial cell fates (see below).

We examined cell proliferation and apoptosis in β-gal^{+} cap mesenchyme-derived cells in the nephrogenic zone at 12.5, 13.5 and 15.5 dpc using phospho-histone H3 (PHH3) and cleaved caspase-3 (CC3) (Fig 3I–L). A significant reduction of PHH3^{+} cells among β-gal^{+} cells was observed at 12.5 dpc (0.51 fold; 29.0 ± 5.63 % in controls and 14.7± 0.73 % in *Pax2* CM

KO) (Fig 3M). Subsequently, a significant increase in $CC3^+$ β-gal^+ cells was observed in the nephrogenic zone at 13.5 dpc (8.95 fold; 0.58 ± 0.90 % in controls and 5.18 ± 0.58 % in *Pax2* CM KO) (Fig 3N). These data suggest that *Pax2* function is also required for normal proliferation and survival of a subset of cap mesenchyme cells and their descendant cells during early stages of kidney development, although we cannot exclude the possibility that the partial defects in cell proliferation and survival are secondary effects caused by the ectopic cell fate change.

Cap mesenchyme cells lacking *Pax2* function can transdifferentiate into renal interstitial progenitors and inner renal medullary interstitial cells

To determine cell types of the *Pax2*-deficient cap mesenchyme-derived cells, we examined cell type marker expression in β-gal^+ cells in *Pax2* CM mutant kidneys at 18.5 dpc (Fig 4A,B). All cap mesenchyme markers examined, including SIX2, CITED1, CDH2 (N-cadherin) and ITGA8 (integrin α8), were not detected in the cortical region of *Pax2* CM mutant kidneys (Fig 4C–F,S3A–H), suggesting that *Pax2*-deficient cap mesenchyme cells failed to maintain the cap mesenchyme status. Further, no $KRT^{-\text{ or low}}$ LAM^+ $CDH1^+$ differentiating nephron epithelial cells were detected in *Pax2* CM mutants (Fig 4G,H and data not shown), indicating a failure of the expected mesenchymal to epithelial transition (MET) of differentiating cap mesenchyme-derived cells during nephron differentiation.

Analysis of FOXD1 as a marker of renal interstitial progenitor cells showed some *Pax2*-deficient cap mesenchyme-derived cells expressing cytoplasmic β-gal also ectopically express FOXD1 in the nucleus at a low level at 13.5 and 15.5 dpc (Fig 4I–L). At 18.5 dpc in *Pax2* CM mutant kidneys, some β-gal^+ cap mesenchyme-derived cells showed higher FOXD1 in the cortical region (Fig 4M,N) and some maintain lower FOXD1 expression in the medullary region (Fig 4O,P). These β-gal^+ $FOXD1^+$ cells in *Pax2* CM mutants also expressed PDGFRB at low levels (Fig S3I–J″), indicating that these cells are not $FOXD1^+$ $PDGFRB^-$ podocytes (Brunskill et al., 2011; Kobayashi et al., 2014). Thus, our data suggest that *Pax2*-deficient cap mesenchyme cells can differentiate into $FOXD1^+$ $PDGFRB^{low}$ renal cortical stroma cells.

Some of the β-gal^+ interstitial cells were $FOXD1^-$ at each stage examined suggesting this population may represent a distinct interstitial cell fate (red arrowheads in Figure 4J,L,P and data not shown). At 18.5 dpc, PDGFRB was expressed broadly in the renal interstitium of control kidneys (Fig 2G,4Q), VIM was expressed in the renal capsule, renal cortical and medullary interstitium (Fig 2O,O′,O″,4S), ITGA8 was highly expressed in the cap mesenchyme in the nephrogenic zone as well as the inner renal medullary interstitium (Fig S3E,G), and CDKN1C (also known as P57KIP2) was observed in a subset of inner renal medullary interstitial cells around the collecting duct system (Fig 4U) and maturing podocytes. In the medullary region of control kidneys, β-gal^+ cap mesenchyme-derived cells contributed to the nephron epithelia, but did not contribute to the renal interstitium, including the $PDGFRB^+$, VIM^+, $ITGA8^+$ $CDKN1C^{+\text{ or }-}$ inner renal medullary interstitium (Fig 4Q,S,U,S3G). In *Pax2* CM mutant kidneys at 18.5 dpc, β-gal^+ cap mesenchyme-derived cells contributed to $PDGFRB^+$, VIM^+, $ITGA8^+$ $CDKN1C^{+\text{ or }-}$ inner renal medullary interstitial cells (Fig 4R,T,V,S3H). Further, PDGFRB, VIM and CDKN1C expression was

already observed in some β-gal$^+$ cap mesenchyme-derived cells in *Pax2* CM mutants at 15.5 dpc (Fig S3K–P). Taken together, these observations suggest that some *Pax2*-deficient cap mesenchyme cells can change cell fate into renal interstitial cell types expressing markers for the cortical stroma and inner renal medullary interstitium.

Transdifferentiation of *Pax2*-deficient cap mesenchyme cells into renal interstitial cells is mediated through transient appearance of a SIX2$^+$ FOXD1$^+$ cell type

We next asked what cellular mechanisms mediate the transdifferentiation of *Pax2*-deficient cap mesenchyme cells into renal interstitial cell types. SIX2$^+$ cap mesenchyme and FOXD1$^+$cortical stroma cells may derive from common progenitors, although there is no definitive evidence due to technical difficulties for clonal analysis of limited number of nephrogenic mesenchyme cells at early stages (Mugford et al., 2008). Therefore, one possibility is that SIX2$^+$ FOXD1$^-$ cap mesenchyme cells de-differentiate into SIX2$^-$ FOXD1$^-$ nephrogenic mesenchyme cells followed by re-differentiation into SIX2$^-$ FOXD1$^+$ cortical stroma cells. If this is the case, it is expected that SIX2 and FOXD1 will not be co-expressed in a transdifferentiating cell. Alternatively, a process that is not frequently observed during normal kidney development may mediate the transdifferentiation.

Therefore, we examined SIX2 and FOXD1 expression in β-gal$^+$ cap mesenchyme-derived cells in *Pax2* CM mutants. In control kidneys at 13.5 dpc, detection of a SIX2$^+$ FOXD1$^+$ cells was a very rare event (Fig 5A,C,E) and tracing of almost all β-gal$^+$ cap mesenchyme-derived cells did not detect a contribution of the SIX2$^+$ derivatives to FOXD1$^+$ cortical stroma (Fig 5G). In *Pax2* CM mutant kidneys at the same stage, SIX2$^+$ FOXD1$^+$ double positive cells were abundantly observed (Fig 5B,D,F). All of these SIX2$^+$ FOXD1$^+$ cells were β-gal$^+$ (Fig 5H), indicating their cap mesenchyme origin. These cap mesenchyme-derived SIX2$^+$ FOXD1$^+$ double positive cells were also observed in *Pax2* CM mutants at 15.5 dpc (Fig S3Q–R‴). These data suggest that a cellular pathway that is not frequently seen in normal development mediates the transdifferentiation of *Pax2*-deficient cap mesenchyme cells into renal interstitial cells through transient SIX2$^+$ FOXD1$^+$ double positive cells.

Pax2 function cell autonomously represses renal interstitial cell fates in cap mesenchyme cells throughout kidney development

Although SIX2 expression is largely lost in *Pax2* CM mutant kidneys at 18.5 dpc (Fig 2I,J, 4C,D), we observed *Six2*-GFP expression remained at low levels (Fig S4). One possibility is that the half-life of CreGFP is longer than that of SIX2. It is also possible that *Pax2*-deficient cap mesenchyme-derived cells repressed endogenous SIX2 expression, but not GFP expression from the *Six2-eGFPCre* BAC transgene efficiently. Alternatively, the *Six2-eGFPCre* transgene is activated ectopically in the *Six2*$^-$ renal interstitium of *Pax2* CM mutant kidneys, which would invalidate the fate map analysis of the cap mesenchyme. To exclude the latter possibility, we performed fate map analysis of *Pax2*-deficient cap mesenchyme cells using the inducible *Six2-eGFPCreER*^{T2} mouse allele, which faithfully recapitulates the endogenous *Six2* expression (Kobayashi et al., 2008). Because induction of eGFPCreER^{T2} by tamoxifen often results in mosaic recombination, this approach also allows mosaic analysis for *Pax2* function in the cap mesenchyme (Fig 6A). If *Pax2* function

is required cell-autonomously in cap mesenchyme cells, *Pax2*-deficient cells may transdifferentiate into renal interstitial cell types. If *Pax2* function is non cell-autonomously required, loss of *Pax2* in some cap mesenchyme will be compensated by surrounding $Pax2^{+}$ cells, resulting in retention of the cap mesenchyme identity in *Pax2*-deficient cells.

We injected 2 mg of tamoxifen into dams at 12.5 dpc and examined β-gal activity in $Six2^{eGFPCreERT2/+}; Pax2^{flox/del}; R26R^{lacZ/+}$ mutant embryos (mosaic *Pax2* CM KO) at 15.5 dpc; $Six2^{eGFPCreERT2/+}; Pax2^{flox/+}; R26R^{lacZ/+}$ littermates were used as controls. At this stage, β-gal^{+} cells were observed in a subset of cap mesenchyme cells in the nephrogenic zone of both controls and mosaic *Pax2* CM mutant kidneys at 15.5 dpc (Fig 6B–C′). Although there was variation between embryos, we observed around 30–50% of cap mesenchyme cells were β-gal^{+} in both controls and mosaic *Pax2* CM mutants under these conditions (Fig 6D,E and data not shown). In mosaic *Pax2* CM mutants, most of β-gal^{+} cells showed reduced PAX2 expression and some started to detach from the ureteric tip at this stage (yellow arrowheads in Fig 6E). A small subset of β-gal^{+} cells maintained the normal PAX2 expression level (yellow arrows in Figure 6E), most likely due to unlinked recombination of the *Pax2* flox and *Rosa26-lacZ* alleles.

At the same stage, while SIX2 and FOXD1 expression patterns were largely mutually exclusive in control kidneys, SIX2^{+} FOXD1^{+} double positive cells were abundantly observed in mosaic *Pax2* CM mutant kidneys (Fig 6F–G″). Most of these SIX2^{+} FOXD1^{+} cells in mosaic *Pax2* CM mutants also expressed β-gal (Fig 6F‴,G‴), indicating their cap mesenchyme origin.

Cell tracing at 18.5 dpc showed that β-gal^{+} cells persisted in mosaic *Pax2* CM mutants (Fig 6H,I) but in contrast to control kidneys where β-gal^{+} cells were maintained in the nephrogenic zone of control kidneys, β-gal^{+} cells were reduced in the nephrogenic zone of mosaic *Pax2* CM mutants (Fig 6H′,I′). No PAX2^{-} cells were detected in the CDH2^{+} cap mesenchyme of mosaic *Pax2* CM mutant kidneys (Fig 6J–K′), suggesting that *Pax2* function is cell-autonomously required for cap mesenchyme development. All β-gal^{+} cells in the CDH2^{+} cap mesenchyme also expressed PAX2 in mosaic *Pax2* CM mutants (yellow arrow in Fig 6K′), indicating that the *Pax2* flox allele was not recombined in these β-gal^{+} cap mesenchyme cells due to the unlinked recombination.

In mosaic *Pax2* CM mutants, large aggregates of β-gal^{+} cap mesenchyme-derived cells were observed within the renal interstitium around the border of the renal cortex and outer renal medulla (Fig 6H–I′). All β-gal^{+} cap mesenchyme-derived cells localized in the renal interstitium expressed PDGFRB (Fig 6L–O), suggesting transdifferentiation into renal interstitial cell types. As above, rare β-gal^{+} cells observed in the cap mesenchyme and nephron epithelia that were PDGFRB^{-} resulted from a partial recombination and retain PAX2 expression in PAX2^{+} tissues (Fig 6M,O).

In the interstitial aggregates in mosaic *Pax2* CM mutants at 18.5 dpc, a subset of β-gal^{+} cells expressed VIM (Fig 6P–S), indicating that *Pax2*-deficient cap mesenchyme-derived cells differentiated into multiple cell types. While these β-gal^{+} cells did not express a nephron progenitor marker SIX2, a renal interstitial progenitor marker FOXD1 was ectopically

expressed in a subset of β-gal$^+$ cells within the interstitial aggregates (Fig 6T,U). Examination of LIV2 expression together with FOXD1 further divided the β-gal$^+$ FOXD1$^+$ cells into sub populations; LIV2$^+$ FOXD1$^+$ and LIV2$^-$ FOXD1$^+$ cells (Fig 6V,W). Although boundaries were not strict, there was tendency for LIV2$^+$ FOXD1$^+$, LIV2$^-$ FOXD1$^+$ and LIV2$^-$ FOXD1$^-$ cells to be localized along the cortico-medullary axis within the interstitial aggregate (blue, yellow and red arrowheads in Fig 6W, respectively). These expression patterns in a interstitial aggregate in mosaic *Pax2* CM mutants are reminiscent of interstitial layers in the cortical region of the kidney; the LIV2$^+$ FOXD1$^+$ VIM$^-$ SIX2$^-$ renal capsule, LIV2$^-$ FOXD1$^+$ VIM^{low} SIX2$^-$ nephrogenic interstitium and LIV2$^-$ FOXD1$^-$ VIM$^+$ SIX2$^-$ renal cortical interstitium along the cortico-medullary axis of the kidney (Fig 6P,T,V). In controls, no β-gal$^+$ cell was observed in the interstitium (Fig 6L,N,P,R,T,V). This cell-autonomous *Pax2* function to maintain cap mesenchyme cells by repressing renal interstitial cell fates is required continuously at a later stage of kidney development, 14.5 dpc (Fig S5).

Single cell RNA-seq profiling revealed repression of nephron programs, but activation of renal interstitial programs in *Pax2*-deficient cap mesenchyme-derived cells

The nephron epithelium and renal interstitium are heterogeneous populations containing molecularly distinct cell types. To compare global gene expression profiles of transdifferentiating *Pax2*-deficient cap mesenchyme cells to those in the nephron and interstitial lineages, we performed single cell RNA-seq analysis. By using a single cell strategy we could better define intermediate stages in the transdifferentiation process as well as better characterize the multiple cell types produced by the *Pax2* mutant cells. Using FACS analysis, tdTomato$^+$ *Pax2*-deficient cap mesenchyme-derived cells were isolated from *Six2-eGFPCre$^{tg/+}$; Pax2$^{flox/del}$; R26R-CAGGS$^{tdTomato/+}$* mutant kidneys at 13.5 and 18.5 dpc. Control cells were collected from *Six2-eGFPCre$^{tg/+}$; Pax2$^{flox/+}$; R26R-CAGGS$^{tdTomato/+}$* kidneys at the same stages. For renal interstitial cells, tdTomato$^+$ cells were isolated from *Foxd1$^{eGFPCreERT2/+}$; Pax2$^{flox/+}$; R26R-CAGGS$^{tdTomato/+}$* kidneys at 18.5 dpc following an injection of 2 mg tamoxifen at 11.5 dpc, which labels all cell types in the renal interstitium (Kobayashi et al., 2014).

The single cell RNA-seq data was first used to provide a global view of the altered gene expression profiles of the *Pax2* CM mutant cells. We were particularly interested in their potentially altered cap mesenchyme versus interstitial character. A list of 792 genes that distinguish wild type interstitial cells from wild type cap mesenchyme and its descendant cells at 18.5 dpc was derived ($P < 0.05$, $FC > 3$) and used for hierarchical clustering (Pearson centered, Wards linkage rule) (Fig 7A). At 13.5 dpc the *Pax2*-deficient cap mesenchyme-derived cells showed significant heterogeneity. Most clustered with the control cap mesenchyme-derived cells, showing that they had not yet acquired significant interstitial gene expression. Other cells, however, clustered among the interstitial cells and showed repression of cap mesenchyme markers and activation of interstitial specific genes (asterisk in Fig 7A). At 18.5 dpc almost all of the *Pax2*-deficient cap mesenchyme-derived cells showed a convincing interstitial gene expression signature. Strongly down regulated genes in the *Pax2*-deficient cap mesenchyme-derived cells at 18.5 dpc included *Six2*, *Crym*, and *Eya1*, markers of the cap mesenchyme, while strongly up regulated genes included *Meis1*, *Anxa2*, and *Foxd1*, markers of the interstitium. These results provide a comprehensive

validation of the striking change in character of the *Pax2*-deficient cap mesenchyme-derived cells, diverging to an interstitial cell type.

Principle components analysis of the single cell expression data provided further insight. A PCA plot showed that most control cap mesenchyme-derived cells at 13.5 dpc had similar gene expression profiles (Fig 7B). Through differentiation into diverse cell types in the nephron epithelium, control cells at 18.5 dpc exhibit showed more diverse gene expression profiles (Fig 7B). Renal interstitial cells at 18.5 dpc had distinct gene expression profiles from control cells in the nephron lineage at 13.5 or 18.5 dpc (Fig 7B). Interestingly, at 18.5 dpc, renal interstitial cells showed larger diversity than the control nephron cells (Fig 7B), indicating that the renal interstitium is a highly heterogeneous population at this stage.

Many *Pax2*-deficient cap mesenchyme-derived cells at 13.5 dpc showed gene expression profiles intermediate between the nephron and renal interstitial cells (Fig 7B). This PCA plot verified that *Pax2*-deficient cells at 18.5 dpc exhibited gene expression profiles much more similar to renal interstitial cells than nephron cells (Fig 7B). Nevertheless, the *Pax2* mutant cells did not show the full heterogeneity of signatures associated with the wild type interstitium, suggesting that they might represent a specific subtype. Of interest, the single cell RNA-seq data showed robust expression of several interstitial type marker genes in the *Pax2*-deficient cap mesenchyme-derived cells. For example, 27 of the top 36 *Vim*$^{+}$ cells in this study, including wild type interstitial cells, were *Pax2*-deficient cap mesenchyme-derived cells. Likewise, ten of the top sixteen *Foxd1*$^{+}$ cells were *Pax2* mutant, with the other six being wild type interstitial cells. The top five cells with the strongest *Acta2*$^{+}$ were all *Pax2* mutant. Nevertheless, as measured by global gene expression patterns, the *Pax2* mutant cells did not clearly fall within any of the wild-type interstitial *Foxd1*$^{+}$, *Vim*$^{+}$, *Tnc*$^{+}$ or *Acta2*$^{+}$ subtypes (data not shown).

The top 100 genes that discriminate the multiple single cell sample types were identified using AltAnalyze (Salomonis et al., 2010) (Fig 7C). The most highly differentially expressed gene was *Xist*, an X-chromosome inactivation gene (Fig 7C), simply reflecting the different sexes of embryos used. The remaining genes were largely classified into two major groups. The most discriminating category contained genes up-regulated in *Pax2*-mutant cells compared to control cells and also highly expressed in the interstitial cells (41 genes out of the 99 genes; 41.4%) (Fig 7C); 17 genes (17.2%) and 24 genes (24.2%) were up-regulated in *Pax2*-mutant cells by 13.5 and 18.5 dpc, respectively (highlighted in pink and orange in Fig 7C). Among these genes, high-quality expression data were available for 35 genes in the GenePaint, Euroexpress and GUDMAP databases (Diez-Roux et al., 2011; Harding et al., 2011; Visel et al., 2004). These expression data confirmed expression patterns in the renal interstitium for 33 genes (94.3%) including collagens (*Col1a1*, *Col3a1* and *Col1a2*), *Anxa2* and *Dcn* (decorin) (Fig S6A,B) (Brunskill et al., 2014; Fetting et al., 2014). These data indicate that renal interstitial genes were up-regulated in the *Pax2*-mutant cells.

Expression of some genes (*Ccnd2* and *Meis1*) was down-regulated in the control cells but high in the interstitial cells at 18.5 dpc (highlighted in green in Fig 7C). Expression of these genes was maintained in the *Pax2* mutant cells at 13.5 and 18.5 dpc (Fig 7C), indicating that

the repression of their expression observed during nephron differentiation did not occur in *Pax2*-deficient cap mesenchyme cells.

Eya1 is specifically expressed in the nephron lineage, but not in the renal interstitium (Xu et al., 2014). Interestingly, *Eya1* expression is lost at 13.5 dpc in mutants (highlighted in yellow in Fig 7C), indicating that *Pax2* function is required for *Eya1* expression in nephron progenitor cells.

The second major category in the top 99 genes contained 50 genes (50.5%) that were down-regulated in *Pax2* mutants at 13.5 dpc and highly repressed at 18.5 dpc compared with high expression in both the control and interstitial cells (highlighted in blue in Fig 7C). In this category, 39 genes (78.0%) were associated with components involved in cell division; cell cycle regulation (*Cks2, Ube2c, Cdk1, Cdca3, Cdca8, Cdca2, Ccnb1, Prc1* and *Ccna2*) (Bertoli et al., 2013; Jiang et al., 1998; Lara-Gonzalez et al., 2012; Walker, 2001), histone structure (*Hist* cluster genes), condensins (*Smc4, Top2a, Ncaph, Smc2* and *Ncapg*) (Hirano, 2012), centromere assembly (*Mis18bp1, Cenpe* and *Cenpa*) (McKinley and Cheeseman, 2016), mitotic spindle assembly checkpoint at the kinetochore (*Spc25, Mad2l1, Nuf2* and *Ndc80*) (Cheeseman and Desai, 2008; Foley and Kapoor, 2013; Lara-Gonzalez et al., 2012), attachment of the mitotic spindle to the centromere (*Aurkb*) (Carmena et al., 2009), spindle microtubule organization (*Tpx2* and *Nusap1*) (Neumayer et al., 2014; Raemaekers et al., 2003), transport along the microtubule (*Kif15, Kif22, Kif11, Kif20a, Kif20b* and *Kif23*) (Hirokawa et al., 2009), and cell proliferation as an antigen identified by antibody Ki-67 (*Mki67*). Among the 50 genes, the public databases contained expression patterns for 36 genes and all (100.0%) were highly expressed in the nephrogenic zone (Fig S6C), where cell proliferation is the most active in the developing kidney (Saifudeen et al., 2002).

As described above, in the cap mesenchyme-specific *Pax2* mutants, loss of the cap mesenchyme causes loss of the nephrogenic zone, leading to arrest of kidney growth around 12.5 dpc (Fig 2A–F), consistent with the reduced cell proliferation at the same stage (Fig 3M). Reduced cell division partially explains the differences in the gene expression profiles for the *Pax2*-mutant cells and renal interstitial cells. It is clear, however, at the global level, the *Pax2*-deficient cap mesenchyme-derived cells undergo a dramatic shift, transforming towards an interstitial identity (Fig 7). Taken together, our observations suggest that *Pax2* function represses a renal interstitial cell program in nephron progenitor cells.

DISCUSSION

Pax2 function in nephron progenitor cells

Pax2 is expressed in multiple tissues in the developing kidney and has been regarded as a key regulator of kidney development since its cloning 25 years ago (Dressler et al., 1990). Consistent with this view, *Pax2* is required for nephric (Wolffian) duct development prior to the onset of kidney (metanephros) development (Bouchard et al., 2002; Torres et al., 1995). Further, human mutations in *PAX2* are associated with kidney anomalies (Sanyanusin et al., 1995). However, despite extensive molecular studies on *Pax2* function, there has been no study specifically addressing *Pax2*'s possible role within the nephron progenitor pool. The conditional *Pax2* null allele reported here gives new insights into *Pax2* function by providing

a useful genetic model for broadly assessing the temporal and spatial action of *Pax2* in potentially any organ system.

Our previous cell fate analysis highlighted specific multipotent progenitor populations for the nephron epithelium and renal interstitium within the ureteric branch tip niche that drives kidney assembly: *Six2*$^{+}$ cap mesenchyme defines a self-renewing nephron progenitor pool and the more peripherally positioned *Foxd1*$^{+}$ population defines a self-renewing renal interstitial progenitor pool (Kobayashi et al., 2014; Kobayashi et al., 2008). Fate mapping also demonstrated that these are mutually exclusive cell populations shortly after the initiation of metanephric kidney organogenesis, indicating a lineage boundary between nephron forming epithelia and renal interstitial compartments of the developing kidney (Kobayashi et al., 2014). Our findings herein suggest that *Pax2* function in nephron progenitor cells is required to maintain the nephron epithelia-interstitium lineage boundary by repressing an alternative renal interstitium-forming pathway cell-autonomously (Fig S7). Thus, *Pax2* is a key transcriptional factor in nephron specification, most likely acting in conjunction with several other transcriptional regulators critical for the nephron progenitor state (Hendry et al., 2011; O'Brien and McMahon, 2014). With kidney disease, the nephrons are lost while the renal interstitium expands (Humphreys et al., 2010). Modulating the action of *Pax2* in interstitial cell lineages could have value in developing regenerative strategies to treat kidney disease by overcoming the lineage boundary segregating the nephron and renal interstitial compartments.

Maintenance of the nephron progenitor status

While there are several factors regulating proliferation and survival of nephron progenitor cells (Barak et al., 2012; Blank et al., 2009; Couillard and Trudel, 2009; Kanda et al., 2014), only a few factors are known to maintain the nephron progenitor status. The *Six2* gene cell-autonomously maintains cap mesenchyme cells by repressing precocious differentiation into mature nephron epithelial cell types (Fig S7) (Kobayashi et al., 2008; Park et al., 2012; Self et al., 2006). Recently, it was shown that EYA1 interacts with SIX2 in nephron progenitor cells during this process (Xu et al., 2014). Inactivation of *Six2* or *Eya1* in the cap mesenchyme results in ectopic formation of nephrons on the cortical side of ureteric tip (Kobayashi et al., 2008; Self et al., 2006; Xu et al., 2014). Although *Pax2* also maintains the nephron progenitor status, its genetic mechanism is novel. *Pax2* function maintains nephron progenitor cells mainly by suppressing transdifferentiation into renal interstitial cell types whereas *Six2* predominantly acts to block commitment to mature nephron cell types (Fig S7).

Pax2-deficient cap mesenchyme cells lose cap mesenchyme status as they detach from the ureteric tip. It is thought that the ureteric tip provides a niche for nephron progenitor cells (Barak et al., 2012; Karner et al., 2011). One possibility is that *Pax2* directly regulates genes essential for the nephron progenitor state, loss of which may cause the detachment from the ureteric tip. Alternatively, *Pax2* function in nephron progenitor cells may regulate cell adhesion to the ureteric tip niche. It is also possible that *Pax2* represses activation of genes specific to interstitial cells, which are located distantly from the ureteric tip. Our studies cannot address whether PAX2 acts as a transcriptional activator and/or repressor in nephron

progenitor cells (Abraham et al., 2015). Future studies will distinguish these alternative mechanisms.

Transdifferentiation of *Pax2*-deficient nephron progenitor cells into renal interstitial cell types

Transdifferentiation can be observed in some genetic mutants and during regeneration after injury. Some transdifferentiation processes are mediated by de-differentiation followed by re-differentiation, and some by artificial events (Jopling et al., 2011). Our observations suggest that transdifferentiation of *Pax2*-deficient nephron progenitor cells into renal interstitium-like cells unfolds in a process involving a transient population of $SIX2^+$ $FOXD1^+$ cells that are not frequently observed during normal kidney development, although possible involvement of partial de- and re-differentiation cannot be excluded.

Interestingly, during mammalian development, mis-regulation of some *Pax* genes can cause transdifferentiation from one lineage to another in various progenitor cells, including *Pax4* function for α and β/γ cell lineages during pancreas development (Collombat et al., 2009; Sosa-Pineda et al., 1997), *Pax5* for B and T cell lineages during lymphocyte development (Cobaleda et al., 2007) and *Pax6* for multiple neuroretinal lineages from the amacrine cell lineage during eye development (Marquardt et al., 2001). One of the common roles for *Pax* genes might be cell lineage specification in progenitor cells during mammalian development, including *Pax2* in nephron progenitor cells during kidney development as we described. Our single cell RNA-seq data suggested that transdifferentiated renal interstitium-like cells derived from *Pax2*-null nephron progenitor cells had somewhat different gene expression profiles from those in endogenous renal interstitial cells, probably because ectopically localized *Pax2*-mutant cells in an abnormal kidney cannot proliferate normally and/or fully differentiated into the mature renal interstitial cells.

Heterogeneity during formation of renal interstitial cell types

Molecular marker analysis showed considerable heterogeneity in the renal interstitium. In *Pax2* CM mutants, not all renal interstitial cell types were observed, likely suggesting that loss of nephrons and arrested ureteric branching may affect renal interstitial differentiation.

An ectopic interstitial aggregate in mosaic *Pax2* CM mutants contains both β-gal^+ and β-gal^- cells, suggesting that multiple cells aggregated when surrounded by more medullary interstitial cell types. It is possible that different renal interstitial cell types have distinctive cell adhesion properties, which may contribute to formation of interstitial layers along the cortico-medullary axis during kidney development.

Currently, it is unclear why *Pax2*-deficient cap mesenchyme cells transdifferentiated into a subset of the renal interstitium. When *Pax2* is inactivated around ~11.0 dpc by the *Six2-eGFPCre* BAC transgene, *Pax2*-deficient cap mesenchyme cells transdifferentiated mainly into renal interstitial cells expressing markers for the nephrogenic and inner renal medullary interstitium. When *Pax2* is inactivated at 12.5 dpc by the *Six2-eGFPCreER^{T2}* knock-in allele, *Pax2*-deficient cap mesenchyme cells transdifferentiated into renal interstitial cells expressing more cortical renal interstitial markers for the renal capsule, nephrogenic interstitium and renal cortical interstitium. We previously showed that the medullary

interstitium starts to differentiate at early stages of kidney development and the cortical interstitium differentiation initiates at later stages (Kobayashi et al., 2014). It is possible that renal interstitial cell precursors derived from FOXD1^{+} cortical stroma progenitors remain multipotent initially. The niche for renal interstitial cell precursors may be dynamic and directs different renal interstitial cell fates in a stage-dependent manner during kidney development. However, the cortico-medulla axis is correctly maintained in vestigial kidneys with arrested development in *Pax2* CM mutants and in an ectopic interstitial aggregate in mosaic *Pax2* CM mutant kidneys. It is also possible that there may be an external positional signal regulating the cortico-medulla axis in the renal interstitium. Further investigation should clarify how multiple renal interstitial cell types are specified and organized in the cortico-medullary layers during kidney development.

STAR★METHODS

KEY RESOURCES TABLE

Please see the separately uploaded file.

CONTACT FOR REAGENT AND RESOURCE SHARING

Further information and requests for resources and reagents should be directed to and will be fulfilled by the Lead Contact, Akio Kobayashi (akiok@uw.edu).

EXPERIMENTAL MODEL AND SUBJECT DETAILS

Mouse strains—All procedures were in accordance with the NIH Guide for the Care and Use of Laboratory Animals and were approved by Institutional Animal Care and Use Committees at Harvard Medical School and the University of Washington. All mice were housed in specific pathogen free (SPF) colonies within vivaria.

Six2-eGFPCre BAC transgenic mice (Kobayashi et al., 2008) and *Six2-eGFPCreER^{T2}* knock-in mice (Kobayashi et al., 2008) were maintained on a CD-1 × Swiss Webster (Taconic) × C57BL/6J (Jackson Laboratory) mixed background and a 129/Sv × C57BL/6J mixed background, respectively, as previously described (Kobayashi et al., 2008). *Rosa26R-lacZ* Cre reporter (*R26R-lacZ*) mice (Soriano, 1999) were purchased from Jackson Laboratory and maintained on a C57BL/6J congenic background using a previously described genotyping methods (Kobayashi et al., 2008). *Rosa26-Flpe* mice (Farley et al., 2000) were purchased from Jackson Laboratory and maintained on a C57BL/6J × 129/Sv mixed background using a genotyping method with the following primers; Flpe-Fw4: AGCATCATGTGCTGCTGAACTAACCTA, Flpe-Rv3: GCTTATGATAGTATTATAGCTCATGAA, R26-Fw11: CTCCCAAAGTCGCTCTGAGTTGTTATCAGT and R26-Rv12: CTCGGGTGAGCATGTCTTTAATCTACCT, which gives a 103-bp band for the *Rosa26-Flpe* allele (Flpe-Fw4 and Flpe-Rv3) and a 484-bp band for the *Rosa26* wild-type allele (R26-Fw11 and R26-Rv12). *Sox2-Cre* mice (Hayashi et al., 2002) were maintained on a C57BL/6J × CBA/J mixed background using a genotyping method with the following primers; Cre-Fw13; GGGGCAATGGTGCGCCTGCTGGAAGAT and rbglobin-pA-Rv1;

CCTTTATTAGCCAGAAGTCAGATGCTCA, which gives a 220-bp band for the *Sox2-Cre* allele (Cre-Fw13 and rbglobin-pA-Rv1).

The *Pax2* flox mouse allele was generated as follows. A *Pax2* targeting vector was constructed using sequence-confirmed homologous arms sub-cloned by PCR from a BAC clone RP23-228G11 containing the *Pax2* locus. *lox*P sites were introduced in PCR primers. An FRT-PGKneobpA-FRT selection cassette (Kobayashi et al., 2008) was introduced following the second *lox*P site. Detailed description of the targeting strategy is available upon a request. Gene targeting and blastocyst injection were performed as previously described (Behringer et al., 2013; Kobayashi et al., 2008). The FRT-PGKneobpA-FRT selection cassette was removed by breeding with *Rosa26-Flpe* mice (Farley et al., 2000). *Pax2* flox mice were maintained on a 129/Sv × C57BL/6J mixed background. *Pax2* flox mice were crossed with *R26R-lacZ* and maintained on a 129/Sv × C57BL/6J mixed background. To generate $Pax2^{del}$ allele, *Pax2* flox mice were crossed with $Sox2\text{-}Cre^{tg/tg}$ mice (Hayashi et al., 2002) maintained on a CBA × C57BL/6J mixed background.

The *Pax2* flox and del mouse allele was genotyped using the following primers; mPax2-Fw29: GGCGCAGGCGGGTTTCTAGTCCGCAGCAGT, mPax2-Rv30: GTGGCTTGGTGGGCGGTCCGGATAGAGGAT, and mPax2-Rv31: ATACCTCCTTTTCTGAATGTAGCTGCCTT, which gives a 288-bp band for the *Pax2* wild-type allele (mPax2-Fw29 and mPax2-Rv30), a 334-bp band for the *Pax2* flox allele (mPax2-Fw29 and mPax2-Rv30) and a 403-bp band for the *Pax2* del allele (mPax2-Fw29 and mPax2-Rv31).

To inactivate *Pax2* in the cap mesenchyme, $Pax2^{flox/flox}$ or $Pax2^{flox/flox}; R26R^{lacZ/lacZ}$ females were mated with $Six2\text{-}eGFPCre^{tg/+}; Pax2^{del/+}$ or $Six2^{eGFPCreERT2/+}; Pax2^{del/+}$ males. Littermates were used for controls. Mice were bred using timed-mating, noon on the day of vaginal plug detection considered 0.5 day post coitum (0.5 dpc). For induction of the $eGFPCreER^{T2}$ protein, tamoxifen (Sigma-Aldrich, T5648) was dissolved in corn oil (Sigma-Aldrich, C8267; Integra Chemical, C819.31) and administrated to dams by intraperitioneal (IP) injection (Danielian et al., 1998).

METHOD DETAILS

Histology—Histology of kidneys was performed as described previously (Kobayashi et al., 2008). Briefly, dissected kidneys were fixed in 4% paraformaldehyde for 1 hr at 4 °C and soaked in 30% sucrose overnight at 4 °C. After embedding in OCT (Sakura, 4583), cryosections were generated at 16 μm using a Leica CM1510 cryostat. Cryosections were blocked with anti-mouse IgG antibody (Jackson ImmunoResearch, 715-007-003) prior to immunostaining to reduce backgrounds from secondary anti-mouse IgG antibodies.

X-gal staining—X-gal staining was performed as described previously (Kobayashi et al., 2005; Kobayashi et al., 2004). Cryosections were stained with X-gal at 37 °C overnight and counter-stained with 0.2% Eosin-Y (Fisher, 23-245-658). Whole-mount kidneys were fixed in 4% paraformaldehyde for 1 hr at 4 °C and stained at 37 °C overnight for embryonic samples or at 4 °C for 2–3 days for neonate samples.

Immunofluorescence—Sections were incubated with primary antibodies against β-gal (MP Biomedicals, 08559761; Abcam, ab9361), CDH1 (E-cadherin) (Thermo Fisher Scientific, 13-1900), CDH2 (N-cadherin) (BD Biosciences, 610920), CDKN1C (P57KIP2) (Abcam, ab4058), CITED1 (Thermo Fisher Scientific, RB-9219-P0), cleaved caspase-3 (Cell Signaling Technology, 9661S), FOXD1 (Santa Cruz Biotechnology; sc-47585, Lot # A1107 and C2310), GFP (Aves labs, GFP-1020; Abcam, ab290), ITGA8 (integrin α8) (R&D Systems, AF4076), KRT (cytokeratin) (Sigma-Aldrich, C2562; DSHB TROMA-I and TROMA-III), LAM (Laminin) (Sigma-Aldrich, L9393), LIV2 (MBL International, D118-3), LTL (*Lotus tetragonolobus* lectin) (Vector Laboratories, FL-1321), PAX2 (Abcam, ab37129; Abnova, H00005076-M01), PDGFRB (eBiosciences, 14-1402-82), phospho histone H3 (EMD Millipore, 06-570), PODXL (podocalyxin) (R&D Systems, MAB1556), SIX2 (Proteintech, 11562-1-AP), ACTA2 (α-smooth muscle actin) (Sigma-Aldrich, A5228), TNC (tenascin C) (Sigma-Aldrich, T3413), UMOD (Uromodulin, Tamm-Horsfall glycoprotein) (R&D Systems, MAB5175) and VIM (Vimentin) (EMD Millipore, AB5733), and detected by the secondary antibodies with DyLight 488, 549 and 649 (Jackson ImmunoResearch). Sections were stained with Hoechst (Thermo Fisher Scientific, H3570) prior to mounting with Immu-Mount (Fisher, 9990412). Fluorescent images were photographed on a Nikon Eclipse C1si confocal with an 80i fluorescent microscope and a Leica TCS SPE-II confocal system with a DMI 4000 fluorescent microscope.

Single cell RNA-seq—Single cell suspension from embryonic kidneys was prepared as previously described (Kobayashi et al., 2008). FACS purification of tdTomato+ cells was performed using a BD FACSAria II. Following the Fluidigm C1 capture, the individual chambers were microscopically examined for the presence of single cells (Brunskill et al., 2014). The cells were robotically lysed and a series of biochemical reactions will be carried out using the Clontech UltraLow SMARTer amplification chemistry and Illumina/Nextera tagmentation-barcoding, as per Fluidigm recommended protocols. Quality of cDNAs was confirmed using an Agilent 2100 Bioanalyzer. The harvested products were then sequenced and paired end, 75 base reads, by an Illumina HiSeq 2500. The resulting data were analyzed using a combination of GeneSpring (Agilent Technologies), AltAnalyze, ToppGene (Chen et al., 2009), TopCluser (Chen et al., 2013), Cytoscape (Shannon et al., 2003) and STRand (Toonen and Hughes, 2001) programs.

QUANTIFICATION AND STATISTICAL ANALYSIS

For quantification of phospho-histone H3+ (PHH3+) and cleaved caspase-3+ (CC3+) cells in β-gal+ cap mesenchyme-derived cells, data were represented as mean ± SD. Significance was defined using unpaired t-test. Values of n represent number of animals.

DATA AND SOFTWARE AVAILABILITY

The single-cell RNA-seq datasets have been deposited in Gene Expression Omnibus (GEO) under accession number GSE79137.

Supplementary Material

Refer to Web version on PubMed Central for supplementary material.

Acknowledgments

We thank Dr. Kevin Eggan for v6.5 ES cells and Andrew S. Potter for data analysis by AltAnalyze. Work in A.P.M.'s laboratory was supported by a grant from the NIH DK054364. Work in the A.K.'s laboratory was supported by grants from NIH DK094933 and OD021437, Basil O'Connor Starter Scholar Research Award from March of Dimes, Carl W. Gottschalk Research Scholar Grant from American Society of Nephrology, and grants from the Harvard Stem Cell Institute and John H. Tietze Stem Cell Scientist Research Award from the Institute for Stem Cell and Regenerative Medicine at University of Washington.

References

Abraham S, Paknikar R, Bhumbra S, Luan D, Garg R, Dressler GR, Patel SR. The Groucho-associated phosphatase PPM1B displaces Pax transactivation domain interacting protein (PTIP) to switch the transcription factor Pax2 from a transcriptional activator to a repressor. The Journal of biological chemistry. 2015; 290:7185–7194. [PubMed: 25631048]

Alcorn D, Maric C, McCausland J. Development of the renal interstitium. Pediatr Nephrol. 1999; 13:347–354. [PubMed: 10454789]

Barak H, Huh SH, Chen S, Jeanpierre C, Martinovic J, Parisot M, Bole-Feysot C, Nitschke P, Salomon R, Antignac C, et al. FGF9 and FGF20 Maintain the Stemness of Nephron Progenitors in Mice and Man. Developmental cell. 2012; 22:1191–1207. [PubMed: 22698282]

Behringer, R., Gertsenstein, M., Vintersten Nagy, K., Nagy, A., Nagy, KV. Manipulating the mouse embryo : A laboratory manual. Fourth. Cold Spring Harbor Laboratory Press; 2013.

Bertoli C, Skotheim JM, de Bruin RA. Control of cell cycle transcription during G1 and S phases. Nat Rev Mol Cell Biol. 2013; 14:518–528. [PubMed: 23877564]

Bertram JF, Cullen-McEwen LA, Egan GF, Gretz N, Baldelomar E, Beeman SC, Bennett KM. Why and how we determine nephron number. Pediatr Nephrol. 2014; 29:575–580. [PubMed: 24022365]

Blank U, Brown A, Adams DC, Karolak MJ, Oxburgh L. BMP7 promotes proliferation of nephron progenitor cells via a JNK-dependent mechanism. Development (Cambridge, England). 2009; 136:3557–3566.

Bouchard M, Souabni A, Mandler M, Neubüser A, Busslinger M. Nephric lineage specification by Pax2 and Pax8. Genes & development. 2002; 16:2958–2970. [PubMed: 12435636]

Boyle S, Misfeldt A, Chandler KJ, Deal KK, Southard-Smith EM, Mortlock DP, Baldwin HS, de Caestecker M. Fate mapping using Cited1-CreER(T2) mice demonstrates that the cap mesenchyme contains self-renewing progenitor cells and gives rise exclusively to nephronic epithelia. Developmental biology. 2007

Boyle SC, Liu Z, Kopan R. Notch signaling is required for the formation of mesangial cells from a stromal mesenchyme precursor during kidney development. Development (Cambridge, England). 2014; 141:346–354.

Brophy P, Ostrom L, Lang K, Dressler G. Regulation of ureteric bud outgrowth by Pax2-dependent activation of the glial derived neurotrophic factor gene. Development (Cambridge, England). 2001; 128:4747–4756.

Brunskill EW, Georgas K, Rumballe B, Little MH, Potter SS. Defining the molecular character of the developing and adult kidney podocyte. PloS one. 2011; 6:e24640. [PubMed: 21931791]

Brunskill EW, Park JS, Chung E, Chen F, Magella B, Potter SS. Single cell dissection of early kidney development: multilineage priming. Development (Cambridge, England). 2014; 141:3093–3101.

Carmena M, Ruchaud S, Earnshaw WC. Making the Auroras glow: regulation of Aurora A and B kinase function by interacting proteins. Curr Opin Cell Biol. 2009; 21:796–805. [PubMed: 19836940]

Cebrian C, Borodo K, Charles N, Herzlinger DA. Morphometric index of the developing murine kidney. Dev Dyn. 2004; 231:601–608. [PubMed: 15376282]

Cheeseman IM, Desai A. Molecular architecture of the kinetochore-microtubule interface. Nat Rev Mol Cell Biol. 2008; 9:33–46. [PubMed: 18097444]

Chen G, Wu Y, Wu J, Zheng W. TopCluster: A hybrid cluster model to support dynamic deployment in Grid. Journal of Computer and System Sciences. 2013; 79:201–215.

Chen J, Bardes EE, Aronow BJ, Jegga AG. ToppGene Suite for gene list enrichment analysis and candidate gene prioritization. Nucleic acids research. 2009; 37:W305–311. [PubMed: 19465376]

Cobaleda C, Jochum W, Busslinger M. Conversion of mature B cells into T cells by dedifferentiation to uncommitted progenitors. Nature. 2007; 449:473–477. [PubMed: 17851532]

Collombat P, Xu X, Ravassard P, Sosa-Pineda B, Dussaud S, Billestrup N, Madsen OD, Serup P, Heimberg H, Mansouri A. The ectopic expression of Pax4 in the mouse pancreas converts progenitor cells into alpha and subsequently beta cells. Cell. 2009; 138:449–462. [PubMed: 19665969]

Costantini F. Genetic controls and cellular behaviors in branching morphogenesis of the renal collecting system. Wiley Interdiscip Rev Dev Biol. 2012; 1:693–713. [PubMed: 22942910]

Costantini F, Kopan R. Patterning a complex organ: branching morphogenesis and nephron segmentation in kidney development. Developmental cell. 2010; 18:698–712. [PubMed: 20493806]

Couillard M, Trudel M. C-myc as a modulator of renal stem/progenitor cell population. Dev Dyn. 2009; 238:405–414. [PubMed: 19161241]

Danielian PS, Muccino D, Rowitch DH, Michael SK, McMahon AP. Modification of gene activity in mouse embryos in utero by a tamoxifen-inducible form of Cre recombinase. Curr Biol. 1998; 8:1323–1326. [PubMed: 9843687]

Diez-Roux G, Banfi S, Sultan M, Geffers L, Anand S, Rozado D, Magen A, Canidio E, Pagani M, Peluso I, et al. A high-resolution anatomical atlas of the transcriptome in the mouse embryo. PLoS Biol. 2011; 9:e1000582. [PubMed: 21267068]

Dressler GR. Patterning and early cell lineage decisions in the developing kidney: the role of Pax genes. Pediatr Nephrol. 2011; 26:1387–1394. [PubMed: 21221999]

Dressler GR, Deutsch U, Chowdhury K, Nornes HO, Gruss P. Pax2, a new murine paired-box-containing gene and its expression in the developing excretory system. Development (Cambridge, England). 1990; 109:787–795.

Dressler GR, Douglass EC. Pax-2 is a DNA-binding protein expressed in embryonic kidney and Wilms tumor. Proceedings of the National Academy of Sciences of the United States of America. 1992; 89:1179–1183. [PubMed: 1311084]

Farley FW, Soriano P, Steffen LS, Dymecki SM. Widespread recombinase expression using FLPeR (flipper) mice. Genesis. 2000; 28:106–110. [PubMed: 11105051]

Fetting JL, Guay JA, Karolak MJ, Iozzo RV, Adams DC, Maridas DE, Brown AC, Oxburgh L. FOXD1 promotes nephron progenitor differentiation by repressing decorin in the embryonic kidney. Development (Cambridge, England). 2014; 141:17–27.

Foley EA, Kapoor TM. Microtubule attachment and spindle assembly checkpoint signalling at the kinetochore. Nat Rev Mol Cell Biol. 2013; 14:25–37. [PubMed: 23258294]

Harding SD, Armit C, Armstrong J, Brennan J, Cheng Y, Haggarty B, Houghton D, Lloyd-MacGilp S, Pi X, Roochun Y, et al. The GUDMAP database–an online resource for genitourinary research. Development (Cambridge, England). 2011; 138:2845–2853.

Hartman H, Lai H, Patterson L. Cessation of renal morphogenesis in mice. Developmental biology. 2007

Hatini V, Huh S, Herzlinger D, Soares V, Lai E. Essential role of stromal mesenchyme in kidney morphogenesis revealed by targeted disruption of Winged Helix transcription factor BF-2. Genes & development. 1996; 10:1467–1478. [PubMed: 8666231]

Hayashi S, Lewis P, Pevny L, McMahon AP. Efficient gene modulation in mouse epiblast using a Sox2Cre transgenic mouse strain. Mechanisms of development. 2002; 119(Suppl 1):S97–S101. [PubMed: 14516668]

Hendry C, Rumballe B, Moritz K, Little MH. Defining and redefining the nephron progenitor population. Pediatr Nephrol. 2011; 26:1395–1406. [PubMed: 21229268]

Hendry CE, Vanslambrouck JM, Ineson J, Suhaimi N, Takasato M, Rae F, Little MH. Direct transcriptional reprogramming of adult cells to embryonic nephron progenitors. J Am Soc Nephrol. 2013; 24:1424–1434. [PubMed: 23766537]

Herzlinger D, Hurtado R. Patterning the renal vascular bed. Seminars in cell & developmental biology. 2014; 36:50–56. [PubMed: 25128732]

Hirano T. Condensins: universal organizers of chromosomes with diverse functions. Genes & development. 2012; 26:1659–1678. [PubMed: 22855829]

Hirokawa N, Noda Y, Tanaka Y, Niwa S. Kinesin superfamily motor proteins and intracellular transport. Nat Rev Mol Cell Biol. 2009; 10:682–696. [PubMed: 19773780]

Humphreys B, Valerius MT, Kobayashi A, Mugford JW, Soeung S, Duffield JS, McMahon AP, Bonventre JV. Intrinsic Epithelial Cells Repair the Kidney after Injury. Cell stem cell. 2008; 2:284–291. [PubMed: 18371453]

Humphreys BD, Lin SL, Kobayashi A, Hudson TE, Nowlin BT, Bonventre JV, Valerius MT, McMahon AP, Duffield JS. Fate tracing reveals the pericyte and not epithelial origin of myofibroblasts in kidney fibrosis. The American journal of pathology. 2010; 176:85–97. [PubMed: 20008127]

Jiang W, Jimenez G, Wells NJ, Hope TJ, Wahl GM, Hunter T, Fukunaga R. PRC1: a human mitotic spindle-associated CDK substrate protein required for cytokinesis. Molecular cell. 1998; 2:877–885. [PubMed: 9885575]

Jopling C, Boue S, Izpisua Belmonte JC. Dedifferentiation, transdifferentiation and reprogramming: three routes to regeneration. Nat Rev Mol Cell Biol. 2011; 12:79–89. [PubMed: 21252997]

Kanda S, Tanigawa S, Ohmori T, Taguchi A, Kudo K, Suzuki Y, Sato Y, Hino S, Sander M, Perantoni AO, et al. Sall1 maintains nephron progenitors and nascent nephrons by acting as both an activator and a repressor. J Am Soc Nephrol. 2014; 25:2584–2595. [PubMed: 24744442]

Karner CM, Das A, Ma Z, Self M, Chen C, Lum L, Oliver G, Carroll TJ. Canonical Wnt9b signaling balances progenitor cell expansion and differentiation during kidney development. Development (Cambridge, England). 2011; 138:1247–1257.

Kobayashi A, Kwan KM, Carroll TJ, McMahon AP, Mendelsohn CL, Behringer RR. Distinct and sequential tissue-specific activities of the LIM-class homeobox gene Lim1 for tubular morphogenesis during kidney development. Development (Cambridge, England). 2005; 132:2809–2823.

Kobayashi A, Mugford JW, Krautzberger AM, Naiman N, Liao J, McMahon AP. Identification of a multipotent self-renewing stromal progenitor population during mammalian kidney organogenesis. Stem cell reports. 2014; 3:650–662. [PubMed: 25358792]

Kobayashi A, Shawlot W, Kania A, Behringer R. Requirement of Lim1 for female reproductive tract development. Development (Cambridge, England). 2004; 131:539–549.

Kobayashi A, Valerius MT, Mugford JW, Carroll TJ, Self M, Oliver G, McMahon AP. Six2 defines and regulates a multipotent self-renewing nephron progenitor population throughout mammalian kidney development. Cell stem cell. 2008; 3:169–181. [PubMed: 18682239]

Lara-Gonzalez P, Westhorpe FG, Taylor SS. The spindle assembly checkpoint. Curr Biol. 2012; 22:R966–980. [PubMed: 23174302]

LeBleu VS, Taduri G, O'Connell J, Teng Y, Cooke VG, Woda C, Sugimoto H, Kalluri R. Origin and function of myofibroblasts in kidney fibrosis. Nature medicine. 2013; 19:1047–1053.

Lemley KV, Kriz W. Anatomy of the renal interstitium. Kidney international. 1991; 39:370–381. [PubMed: 2062030]

Levinson R, Mendelsohn C. Stromal progenitors are important for patterning epithelial and mesenchymal cell types in the embryonic kidney. Seminars in cell & developmental biology. 2003; 14:225–231. [PubMed: 14627121]

Lin EE, Sequeira-Lopez ML, Gomez RA. RBP-J in FOXD1+ renal stromal progenitors is crucial for the proper development and assembly of the kidney vasculature and glomerular mesangial cells. Am J Physiol Renal Physiol. 2014; 306:F249–258. [PubMed: 24226518]

Little MH, Brennan J, Georgas K, Davies JA, Davidson DR, Baldock RA, Beverdam A, Bertram JF, Capel B, Chiu HS, et al. A high-resolution anatomical ontology of the developing murine genitourinary tract. Gene Expr Patterns. 2007; 7:680–699. [PubMed: 17452023]

Little MH, McMahon AP. Mammalian kidney development: principles, progress and projections. Cold Spring Harb Perspect Biol. 2012; 4

Luyckx VA, Brenner BM. Birth weight, malnutrition and kidney-associated outcomes–a global concern. Nature reviews Nephrology. 2015; 11:135–149. [PubMed: 25599618]

Marquardt T, Ashery-Padan R, Andrejewski N, Scardigli R, Guillemot F, Gruss P. Pax6 is required for the multipotent state of retinal progenitor cells. Cell. 2001; 105:43–55. [PubMed: 11301001]

McKinley KL, Cheeseman IM. The molecular basis for centromere identity and function. Nat Rev Mol Cell Biol. 2016; 17:16–29. [PubMed: 26601620]

Mugford JW, Sipila P, McMahon JA, McMahon AP. Osr1 expression demarcates a multi-potent population of intermediate mesoderm that undergoes progressive restriction to an Osr1-dependent nephron progenitor compartment within the mammalian kidney. Developmental biology. 2008; 324:88–98. [PubMed: 18835385]

Neumayer G, Belzil C, Gruss OJ, Nguyen MD. TPX2: of spindle assembly, DNA damage response, and cancer. Cell Mol Life Sci. 2014; 71:3027–3047. [PubMed: 24556998]

O'Brien LL, McMahon AP. Induction and patterning of the metanephric nephron. Seminars in cell & developmental biology. 2014; 36:31–38. [PubMed: 25194660]

Park J, Valerius M, McMahon A. Wnt/{beta}-catenin signaling regulates nephron induction during mouse kidney development. Development (Cambridge, England). 2007; 134:2533–2539.

Park JS, Ma W, O'Brien LL, Chung E, Guo JJ, Cheng JG, Valerius MT, McMahon JA, Wong WH, McMahon AP. Six2 and Wnt regulate self-renewal and commitment of nephron progenitors through shared gene regulatory networks. Developmental cell. 2012; 23:637–651. [PubMed: 22902740]

Pippin JW, Sparks MA, Glenn ST, Buitrago S, Coffman TM, Duffield JS, Gross KW, Shankland SJ. Cells of renin lineage are progenitors of podocytes and parietal epithelial cells in experimental glomerular disease. The American journal of pathology. 2013; 183:542–557. [PubMed: 23769837]

Quaggin SE, Kreidberg JA. Development of the renal glomerulus: good neighbors and good fences. Development (Cambridge, England). 2008; 135:609–620.

Raemaekers T, Ribbeck K, Beaudouin J, Annaert W, Van Camp M, Stockmans I, Smets N, Bouillon R, Ellenberg J, Carmeliet G. NuSAP, a novel microtubule-associated protein involved in mitotic spindle organization. J Cell Biol. 2003; 162:1017–1029. [PubMed: 12963707]

Ranghini EJ, Dressler GR. Evidence for intermediate mesoderm and kidney progenitor cell specification by Pax2 and PTIP dependent mechanisms. Developmental biology. 2015; 399:296–305. [PubMed: 25617721]

Romagnani P, Lasagni L, Remuzzi G. Renal progenitors: an evolutionary conserved strategy for kidney regeneration. Nature reviews Nephrology. 2013; 9:137–146. [PubMed: 23338209]

Rothenpieler UW, Dressler GR. Pax-2 is required for mesenchyme-to-epithelium conversion during kidney development. Development (Cambridge, England). 1993; 119:711–720.

Saifudeen Z, Marks J, Du H, El-Dahr SS. Spatial repression of PCNA by p53 during kidney development. Am J Physiol Renal Physiol. 2002; 283:F727–733. [PubMed: 12217864]

Salomonis N, Schlieve CR, Pereira L, Wahlquist C, Colas A, Zambon AC, Vranizan K, Spindler MJ, Pico AR, Cline MS, et al. Alternative splicing regulates mouse embryonic stem cell pluripotency and differentiation. Proceedings of the National Academy of Sciences of the United States of America. 2010; 107:10514–10519. [PubMed: 20498046]

Sanyanusin P, Schimmenti LA, McNoe LA, Ward TA, Pierpont ME, Sullivan MJ, Dobyns WB, Eccles MR. Mutation of the PAX2 gene in a family with optic nerve colobomas, renal anomalies and vesicoureteral reflux. Nature genetics. 1995; 9:358–364. [PubMed: 7795640]

Saxen, L. Organogenesis of the Kidney. New York: Cambridge University Press; 1987.

Self M, Lagutin O, Bowling B, Hendrix J, Cai Y, Dressler G, Oliver G. Six2 is required for suppression of nephrogenesis and progenitor renewal in the developing kidney. The EMBO journal. 2006; 25:5214–5228. [PubMed: 17036046]

Sequeira Lopez ML, Gomez RA. Development of the renal arterioles. J Am Soc Nephrol. 2011; 22:2156–2165. [PubMed: 22052047]

Shannon P, Markiel A, Ozier O, Baliga NS, Wang JT, Ramage D, Amin N, Schwikowski B, Ideker T. Cytoscape: a software environment for integrated models of biomolecular interaction networks. Genome Res. 2003; 13:2498–2504. [PubMed: 14597658]

Soriano P. Generalized lacZ expression with the ROSA26 Cre reporter strain. Nature genetics. 1999; 21:70–71. [PubMed: 9916792]

Sosa-Pineda B, Chowdhury K, Torres M, Oliver G, Gruss P. The Pax4 gene is essential for differentiation of insulin-producing beta cells in the mammalian pancreas. Nature. 1997; 386:399–402. [PubMed: 9121556]

Stark K, Vainio S, Vassileva G, McMahon AP. Epithelial transformation of metanephric mesenchyme in the developing kidney regulated by Wnt-4. Nature. 1994; 372:679–683. [PubMed: 7990960]

Stewart K, Bouchard M. Coordinated cell behaviours in early urogenital system morphogenesis. Seminars in cell & developmental biology. 2014; 36:13–20. [PubMed: 25220017]

Taguchi A, Kaku Y, Ohmori T, Sharmin S, Ogawa M, Sasaki H, Nishinakamura R. Redefining the in vivo origin of metanephric nephron progenitors enables generation of complex kidney structures from pluripotent stem cells. Cell stem cell. 2014; 14:53–67. [PubMed: 24332837]

Takasato M, Er PX, Chiu HS, Maier B, Baillie GJ, Ferguson C, Parton RG, Wolvetang EJ, Roost MS, Chuva de Sousa Lopes SM, et al. Kidney organoids from human iPS cells contain multiple lineages and model human nephrogenesis. Nature. 2015; 526:564–568. [PubMed: 26444236]

Toonen RJ, Hughes S. Increased throughput for fragment analysis on an ABI PRISM 377 automated sequencer using a membrane comb and STRand software. Biotechniques. 2001; 31:1320–1324. [PubMed: 11768661]

Torres M, Gómez-Pardo E, Dressler G, Gruss P. Pax-2 controls multiple steps of urogenital development. Development (Cambridge, England). 1995; 121:4057–4065.

Visel A, Thaller C, Eichele G. GenePaint.org: an atlas of gene expression patterns in the mouse embryo. Nucleic acids research. 2004; 32:D552–556. [PubMed: 14681479]

Walker MG. Drug target discovery by gene expression analysis: cell cycle genes. Curr Cancer Drug Targets. 2001; 1:73–83. [PubMed: 12188893]

Xu J, Wong EY, Cheng C, Li J, Sharkar MT, Xu CY, Chen B, Sun J, Jing D, Xu PX. Eya1 interacts with Six2 and Myc to regulate expansion of the nephron progenitor pool during nephrogenesis. Developmental cell. 2014; 31:434–447. [PubMed: 25458011]

HIGHLIGHTS

- *Pax2* represses interstitial fates in nephron progenitor cells of developing kidneys
- *Pax2*-null cells adapt hybrid status of nephron and interstitium progenitor cells
- Nephron progenitor cells lacking *Pax2* differentiate into renal interstitial cells

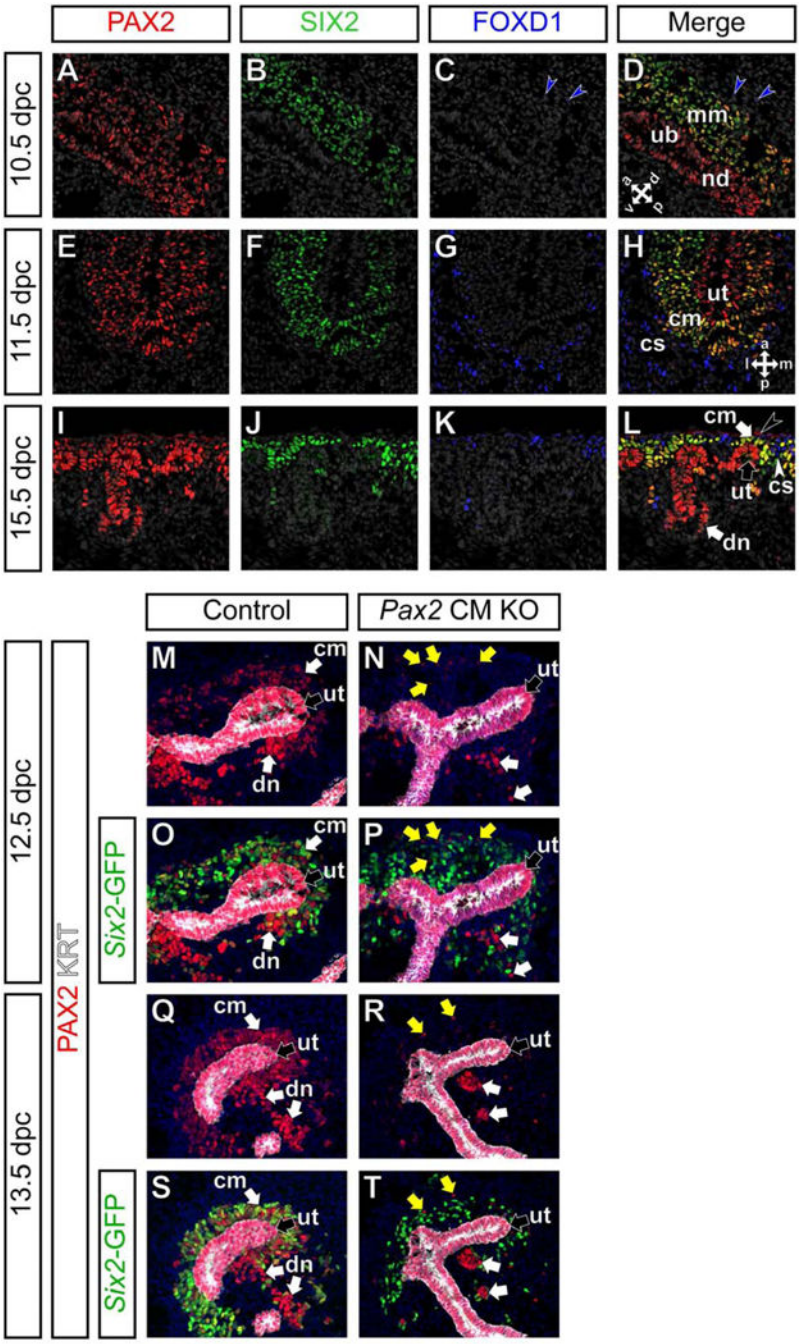

Figure 1. Inactivation of *Pax2* in the cap mesenchyme of the developing kidney

(A–H) Confocal immunofluorescence of wild-type kidneys at 10.5 (A–D), 11.5 (E–H) and 15.5 dpc (I–L) with PAX2 (red), SIX2 (green) and FOXD1 (blue) and Hoechst (gray) staining. Double arrows in D and H indicate anterio-posterior, dorso-ventral or medio-lateral axes. Blue arrowheads in C,D indicate cells expressing FOXD1 at low levels. A black arrowhead in L indicates non-specific (non-PAX2) staining from an anti-mouse IgG secondary antibody, between connective tissue and renal capsule cells. (M–T) Confocal immunofluorescence of the nephrogenic zone of kidneys from *Six2-eGFPCre*$^{tg/+}$*; Pax2*$^{flox/+}$

control (M,O,Q,S) and *Six2-eGFPCre*$^{tg/+}$; *Pax2*$^{flox/del}$ cap mesenchyme-specific *Pax2* knock-out (*Pax2* CM KO) (N,P,R,T) mutant mice with PAX2 (red), *Six2*-GFP (cap mesenchyme; green), cytokeratin (KRT, ureteric tip; white) and Hoechst (nucleus; blue) staining at 12.5 dpc (M–P) and 13.5 dpc (Q–T). PAX2 expression is reduced in the cap mesenchyme surrounding the ureteric tip. Note that the *Six2-eGFPCre* BAC transgene is mosaic in the cap mesenchyme, as previously observed (Kobayashi et al., 2008). Yellow and white arrows in N,P,R,T indicate PAX2^{+} cells that escaped Cre recombination in the cap mesenchyme and differentiating nephron, respectively. cm, cap mesenchyme; cs, renal cortical stroma; dn, differentiating nephron; mm, metanephric mesenchyme; nd, nephric duct; ub, ureteric bud; ut, ureteric tip.

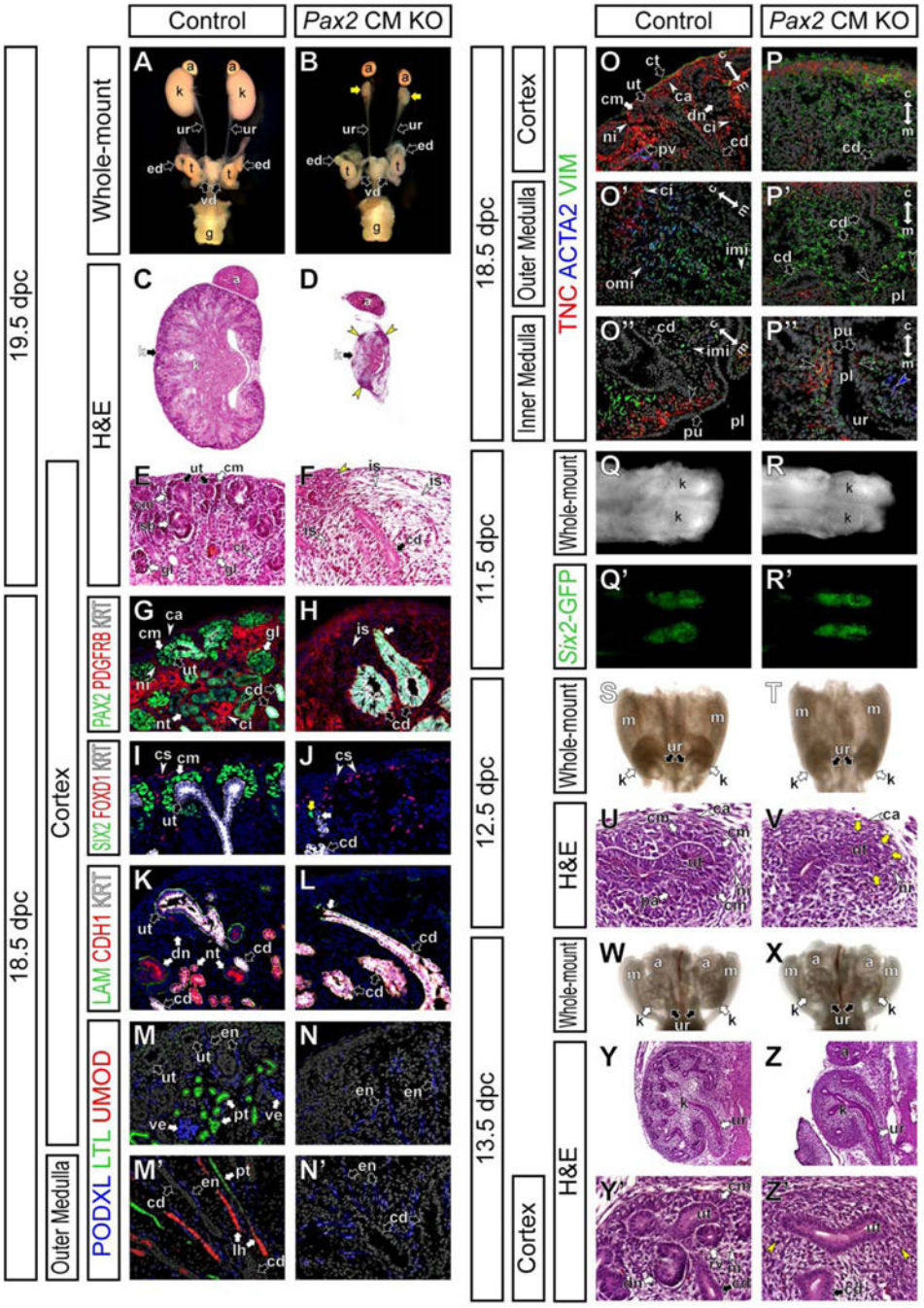

Figure 2. *Pax2* is required for development of the cap mesenchyme

Six2-eGFPCre$^{tg/+}$*; Pax2*$^{flox/+}$ control mice (Control) and *Six2-eGFPCre*$^{tg/+}$*; Pax2*$^{flox/del}$ cap mesenchyme-specific *Pax2* mutant mice (*Pax2* CM KO). (A and B) Whole-mount view of the urogenital system at 19.5 dpc. Yellow arrows in B indicate hypoplastic kidneys. (C and D) H&E stained sections of kidneys at 19.5 dpc. (E and F) High magnification of cortical regions in C and D, respectively. Yellow arrowheads in D and F indicate focal thickened tissues around rare ureteric tips. (G–P″) Confocal immunofluorescence of the renal cortex (G–N,O,P), outer renal medulla (M′,N′,O′,P′) and inner renal medulla (O″,P″) of kidneys

at 18.5 dpc. (G and H) PAX2 (green), PDGFRB (red) and cytokeratin (KRT; white). (I and J) SIX2 (green), FOXD1 (red) and cytokeratin (KRT; white). Yellow and white arrows in J indicate a rare $SIX2^+$ cell and a rare ureteric tip, respectively. (K and L) Epithelial markers; laminin (LAM; green), E-cadherin (CDH1; red) and cytokeratin (KRT; white). (M–N′) Nephron segment markers; podocalyxin (PODXL, podocytes and endothelium; green), *Lotus Tetragonolobus* Lectin (LTL, proximal tubule; red) and Uromodulin (UMOD, loop of Henle; red). (O–P″) Interstitial layer markers; tenascin C (TNC; green), α-smooth muscle actin (ACTA2; blue) and Vimentin (VIM; green). Double arrows indicate the cortico-medullary axis of the kidney. Black arrowheads in O″ and P″ indicate the TNC^+ most inner renal medullary interstitium adjacent to the pelvic urothelial lining (pu). The blue arrowhead in P″ indicates $ACTA2^+$ cells in the ureter mesenchyme. (Q–R′) Dorsal view of the whole-mount posterior urogenital system at 11.5 dpc. (Q and R) Bright view. (Q′ and R′) GFP expression in Q and R, respectively. (S and T) Dorsal view of the whole-mount urogenital system at 12.5 dpc. (U and V) H&E stained sections of the nephrogenic zone of kidneys at 12.5 dpc. Yellow arrows in V indicate less condensed cap mesenchyme cells. (W and X) Dorsal view of the whole-mount urogenital system at 13.5 dpc. (Y–Z′) H&E stained sections of kidneys at 13.5 dpc. (Y and Z) Whole kidneys. (Y′ and Z′) Higher magnification of the nephrogenic zone in Y and Z, respectively. Yellow arrowheads in Z′ indicate interstitium-like tissues directly surrounding the ureteric tip. a, adrenal gland; ca, renal capsule; cd, collecting duct; ci, renal cortical interstitium; cm, cap mesenchyme; dn, differentiating nephron; en, endothelium; ed, epididymis; g, genitalia; gl, glomerulus; is, renal interstitium; imi, inner renal medullary interstitium; k, kidney; lh, loop of Henle; m, mesonephros; ni, nephrogenic interstitium; nt, nephron tubule; omi, outer renal medullary interstitium; pl, pelvis; pt, proximal tubule, pu, pelvic urothelial lining; pv, peri-vasculature; rv, renal vesicle; sb, S-shaped body; t, testis; ur, ureter; ut, ureteric tip; ve, visceral epithelium (podocytes); vd, vas deferens.

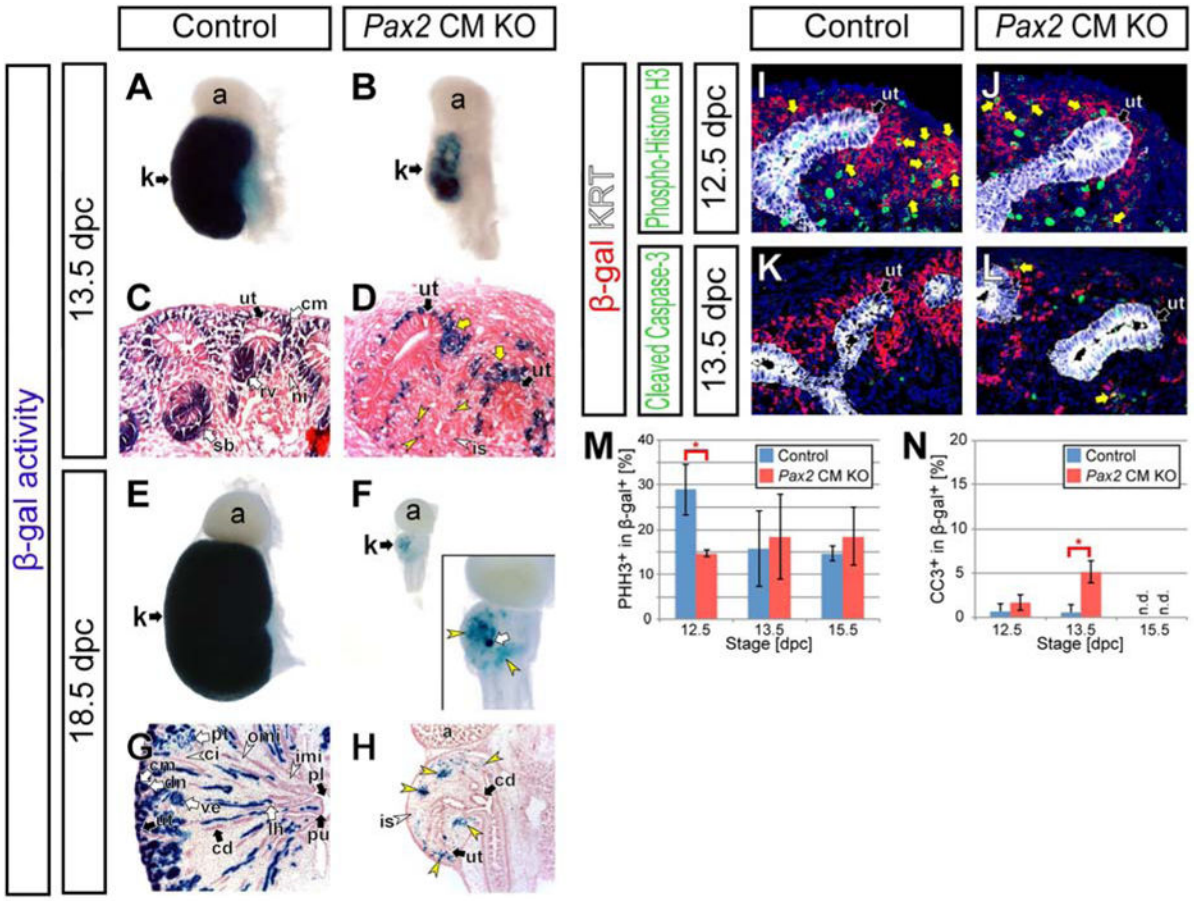

Figure 3. Some *Pax2*-deficient cap mesenchyme cells can persist throughout kidney development

(A–H) Kidneys from *Six2-eGFPCre*$^{tg/+}$; *Pax2*$^{flox/+}$; *R26R*$^{lacZ/+}$ control mice (Control) and *Six2-eGFPCre*$^{tg/+}$; *Pax2*$^{flox/del}$; *R26R*$^{lacZ/+}$ cap mesenchyme-specific *Pax2* mutant mice (*Pax2* CM KO). X-gal staining of whole-mount tissues (A,B,E,F) and sections counter-stained with eosin (C,D,G,H) at 13.5 dpc (A–D) and 18.5 dpc (E–H). Yellow arrows and yellow arrowheads in D indicate β-gal$^+$ cap mesenchyme-derived cells around the ureteric tip with less columnar cell shape and spreading away from the ureteric tip, respectively. The inset in F shows a high magnification of a hypoplastic kidney in *Pax2* CM mutants. Yellow arrowheads and white arrow in F and H indicate β-gal+ cap mesenchyme-derived cells in the interstitium and in a few rare nephrons, respectively. (I–L) Confocal immunofluorescence of the nephrogenic zone of kidneys from Control mice (I,K) and *Pax2* CM KO mice (J,L) with β-gal (red) and cytokeratin (KRT; ureteric tip, white) staining. (I,J) Phospho-histone H3 (green) staining at 12.5 dpc. Yellow arrows indicate β-gal$^+$ phospho-histone H3$^+$ cells. (K,L) Cleaved caspase-3 staining at 13.5 dpc. Yellow arrows in M indicate β-gal$^+$ cleaved caspase-3$^+$ cells. (M and N) Quantification of phospho-histone H3$^+$ (PHH3$^+$) (M) and cleaved caspase-3$^+$ (CC3$^+$) (N) cells in β-gal$^+$ cap mesenchyme-derived cells. Data are represented as mean ± SD. Asterisks indicate $p<0.05$ with unpaired t-test. n.d., not detected. Abbreviations as in Figure 2.

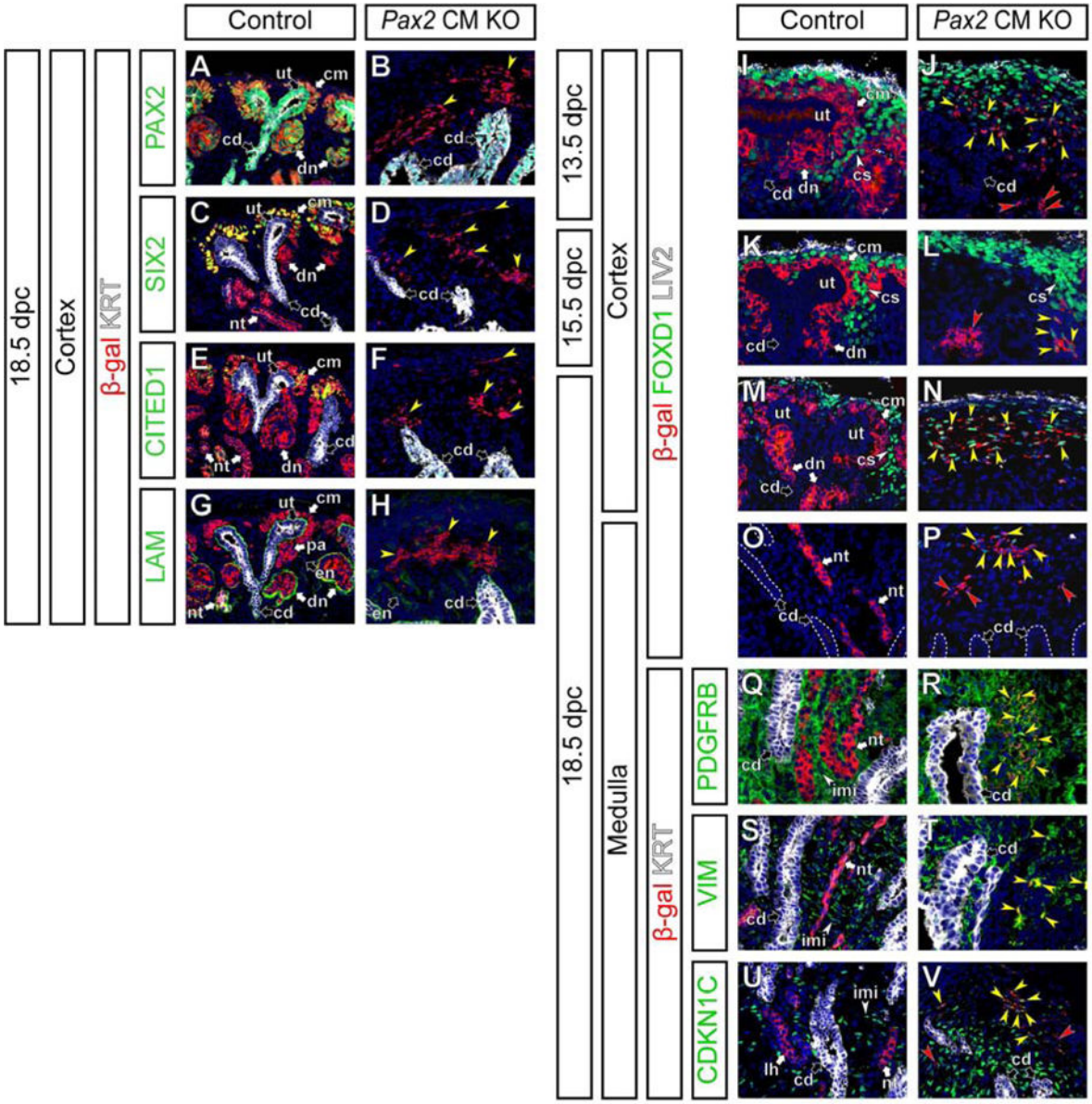

Figure 4. Cap mesenchyme cells lacking *Pax2* function can differentiate into nephrogenic and inner renal medullary interstitial cells

Confocal immunofluorescence of kidneys from Control and *Pax2* CM KO mice with β-gal (cap mesenchyme-derived cells; red) and Hoechst (nucleus; blue) staining. (A–H) Cortical regions at 18.5 dpc with cytokeratin (KRT, ureteric tip and collecting duct; white) with PAX2 (A,B), SIX2 (C,D), CITED1 (E,F) and Laminin (LAM) (G,H) staining in green. Yellow arrowheads in B,D,F,H indicate β-gal^{+} cells without PAX2 expression (B), cap mesenchyme markers (SIX2 in D and CITED1 in F) or nephron tubule makers (LAM^{+} KRT$^{-\text{ or low}}$ in H) in *Pax2* CM mutants. (I–P) Cortical (I–N) and medullary (O,P) regions at 13.5 dpc (I,J), 15.5 dpc (K,L) and 18.5 dpc (M–P) with FOXD1 (cortical stroma; green) and LIV2 (connective tissue and renal capsule; white) staining. Yellow and red arrows in J,L,N,P indicate β-gal^{+} FOXD1^{+} (β-gal in the cytoplasm and FOXD1 in the nucleus) and β-gal^{+} FOXD1^{-} cells, respectively. (Q–V) Medullary regions at 18.5 dpc with cytokeratin (KRT,

collecting duct; white) staining with PDGFRB (Q,R), Vimentin (VIM) (S,T) and CDKN1C (also known as P57KIP2) (U,V) staining in green. Yellow arrowheads in R,T,V indicate cytoplasmic β-gal^{+} cells expressing a interstitial marker (membranous PDGFRB in R, cytoplasmic VIM in T and nuclear CDKN1C in V). Red arrowheads in V indicate β-gal^{+} CDKN1C^{-} cells. Note that not all inner renal interstitial cells express CDKN1C in controls (U). Abbreviations as in Figure 2 and cs, renal cortical stroma; pa, pretubular aggregate.

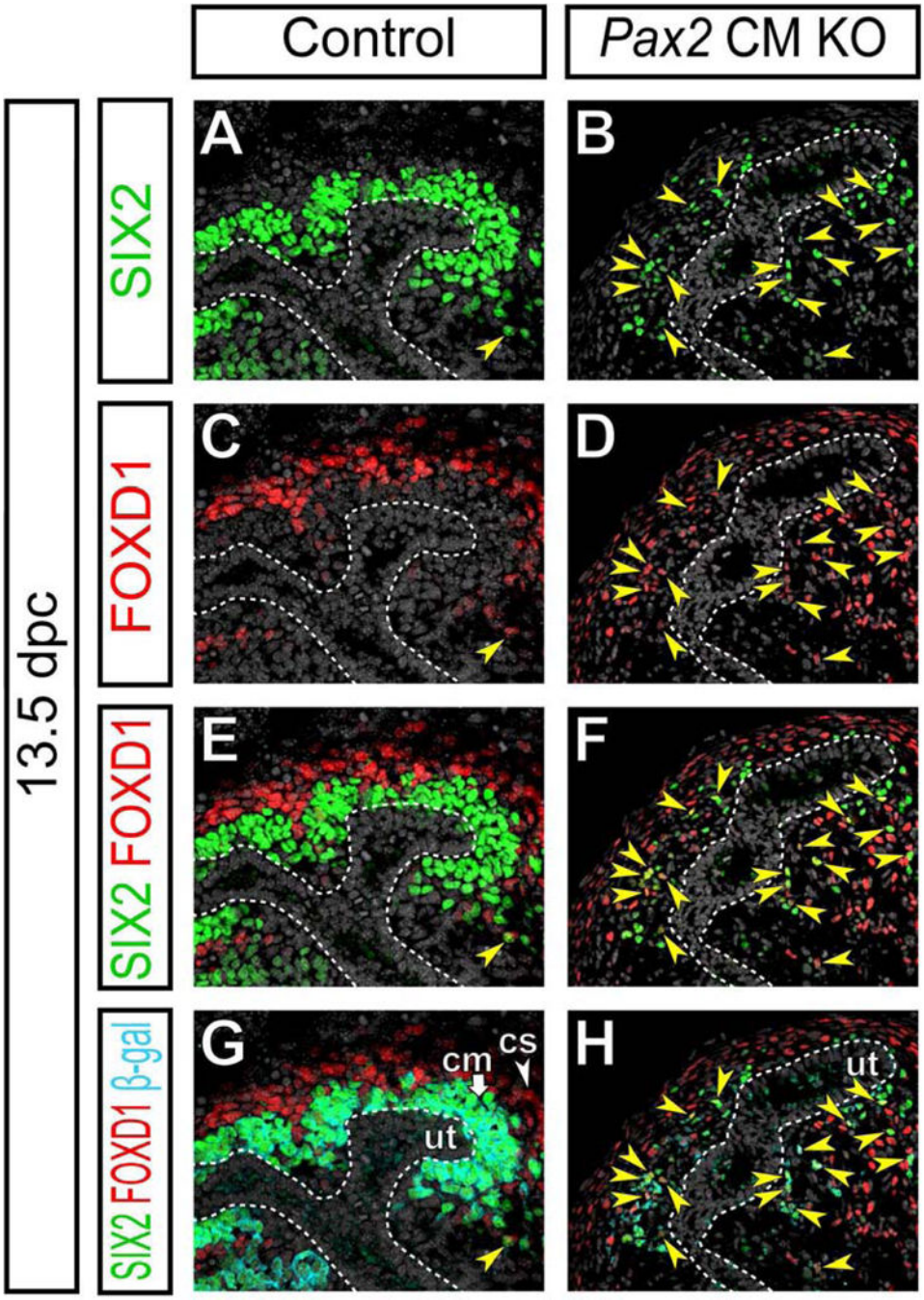

Figure 5. *Pax2*-deficient cap mesenchyme cells transiently become SIX2$^+$ FOXD1$^+$ double positive cells

Confocal immunofluorescence of the cortical region of kidneys from Control and *Pax2* CM KO mice at 13.5 dpc with SIX2 (green), FOXD1 (red), β-gal (cap mesenchyme-derived cells; cyan) and Hoechst (nucleus; gray) staining. Yellow arrowheads and white dotted lines indicate SIX2$^+$ FOXD1$^+$ β-gal$^+$ cells and the collecting duct system, respectively. Abbreviations as in Figure 2.

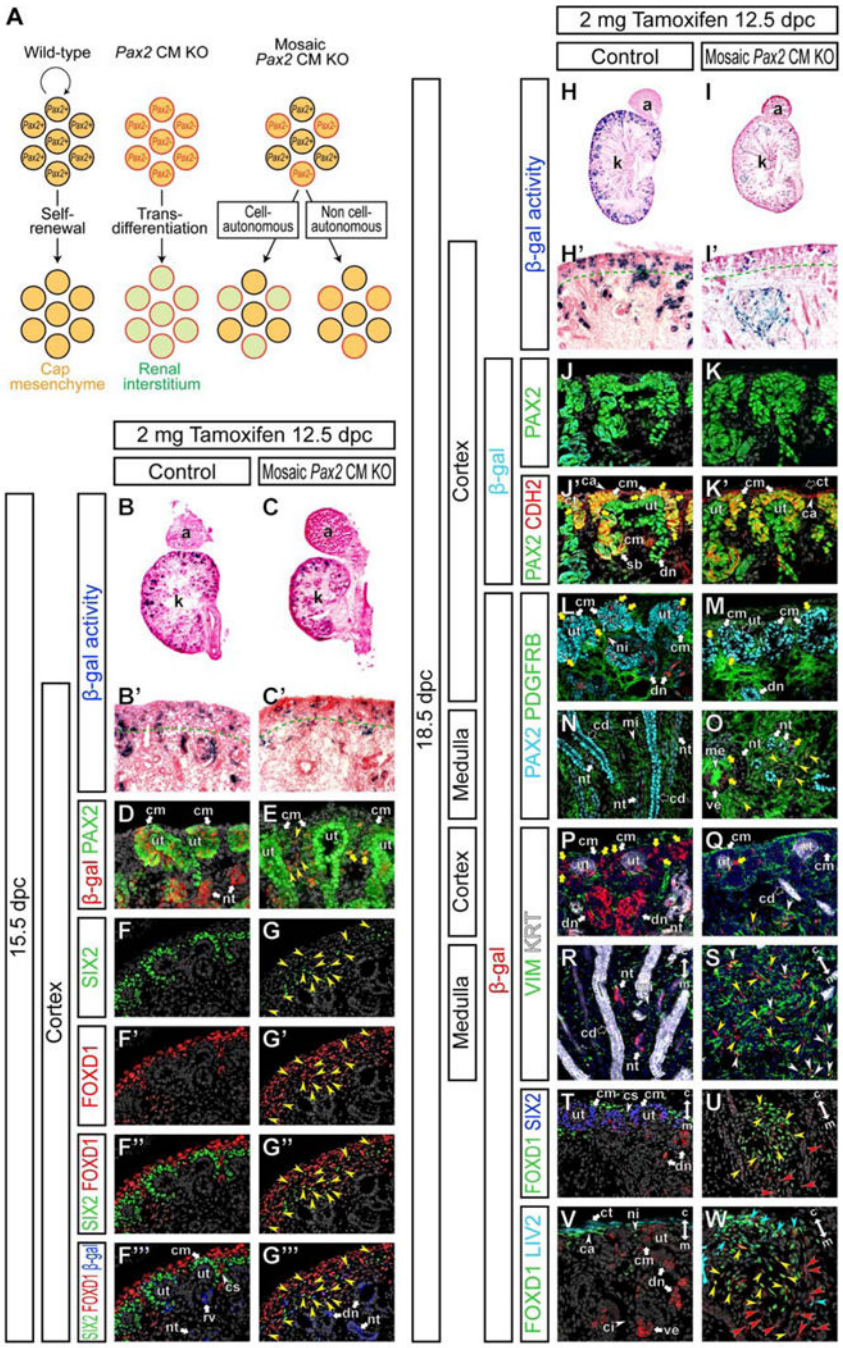

Figure 6. *Pax2* function in cap mesenchyme cells is required cell-autonomously to repress transdifferentiation into renal interstitial cells at a later stage of kidney development

(A) Schematic illustration of mosaic analysis for *Pax2* function in cap mesenchyme cells. In wild-type kidneys, *Pax2* wild-type (black perimeter) cap mesenchyme cells (orange fill) can self-renew. *Pax2*-deficient (red perimeter) cap mesenchyme cells transdifferentiate into renal interstitial cell types (green fill) in the *Pax2* CM mutants. In mosaic cap mesenchyme-specific *Pax2* (mosaic *Pax2* CM) mutants, some cap mesenchyme cells remain $Pax2^{+}$, while the others become $Pax2^{-}$. If *Pax2* function is cell-autonomously required to repress renal interstitial cell fates (1), $Pax2^{-}$ cells will transdifferentiate into renal interstitial cells and

may become excluded from the cap mesenchyme. If *Pax2* function is required non cell-autonomously by regulating secreted factors or membrane-bound molecules signaling extracellularly (2), defects in $Pax2^{-}$ cells will be compensated by surrounding $Pax2^{+}$ cells. Therefore, $Pax2^{-}$ cells will be able to remain as cap mesenchyme cells. (B–W) Kidneys from $Six2^{eGFPCreERT2/+}; Pax2^{flox/+}; R26R^{lacZ/+}$ control mice (Control) and $Six2^{eGFPCreERT2/+}; Pax2^{flox/del}; R26R^{lacZ/+}$ mosaic cap mesenchyme-specific *Pax2* mutant mice (Mosaic *Pax2* CM KO) after injection of 2 mg of tamoxifen into dams at 12.5 dpc. (B and C) X-gal (blue) stained section counter-stained with eosin (pink) at 15.5 dpc. (B′ and C′) High magnification of cortical regions in B and C, respectively. Green dotted lines indicate the boundary between the nephrogenic zone and renal cortex. (D and E) Confocal immunofluorescence of the cortical region of the kidney at 15.5 dpc with β-gal (cap mesenchyme-derived cells; red), PAX2 (green) and Hoechst (nucleus; gray) staining. Yellow arrowheads and yellow arrows in E indicate β-gal^{+} cells with reduced and normal PAX2 expression levels, respectively. (F–G‴) Confocal immunofluorescence of the cortical region of the kidney at 15.5 dpc with SIX2 (green), FOXD1 (red), β-gal (cap mesenchyme-derived cells; blue) and Hoechst (nucleus; gray) staining. Yellow arrowheads indicate SIX2^{+} FOXD1^{+} β-gal^{+} cells. (H and I) X-gal (blue) stained sections counter-stained with eosin (pink) at 18.5 dpc. (H′ and I′) High magnification of cortical regions in H and I, respectively. Green dotted lines indicate the boundary between the nephrogenic zone and renal cortex. (J–W) Confocal immunofluorescence of the kidney at 18.5 dpc with β-gal (cap mesenchyme-derived cells; cyan in J–K′ and red in L–W) and Hoechst (nucleus; gray in J–O,T–W and blue in P–S) staining. (J–K′) The cortical region with PAX2 (green) and N-cadherin (CDH2; red) staining. Yellow arrows in J′,K′ indicate β-gal^{+} PAX2^{+} cells in the CDH2^{+} cap mesenchyme. (L–O) The cortical (L,M) and medullary (N,O) regions with PAX2 (cyan) and PDGFRB (green) staining. Yellow arrows in L,M indicate β-gal^{+} PAX2^{+} cells in the cap mesenchyme. Yellow arrowheads and yellow arrows in O indicate β-gal^{+} PDGFRB^{+} cells and β-gal^{+} cells in the nephron epithelium, respectively. (P–S) The cortical (P,Q) and medullary (R,S) regions with VIM (green) and cytokeratin (KRT; white) staining. Yellow arrows in P,Q, yellow arrowheads and white arrowheads in Q,S indicate β-gal^{+} cells in the cap mesenchyme, and β-gal^{+} VIM^{-} and β-gal^{+} VIM^{+} cells in interstitial aggregates in mosaic *Pax2* CM mutants, respectively. (T–W) Cortical regions (T,V) and interstitial aggregates (U,W) with FOXD1 (green) and SIX2 (blue) (T,U) or LIV2 (cyan) (V,W) staining. Yellow arrowheads in U, β-gal^{+} FOXD1^{+} cells; red arrowheads in U, β-gal^{+} FOXD1^{-} cells. Cyan arrowheads in W, β-gal^{+} FOXD1^{+} LIV2^{+} cells; yellow arrowheads in W; β-gal^{+} FOXD1^{+} LIV2^{-} cells; red arrowheads in W, β-gal^{+} FOXD1^{-} LIV2^{-} cells. Double arrows in R–W indicate the cortico-medullary axis of the kidney. Abbreviations as in Figure 2 and cs, renal cortical stroma.

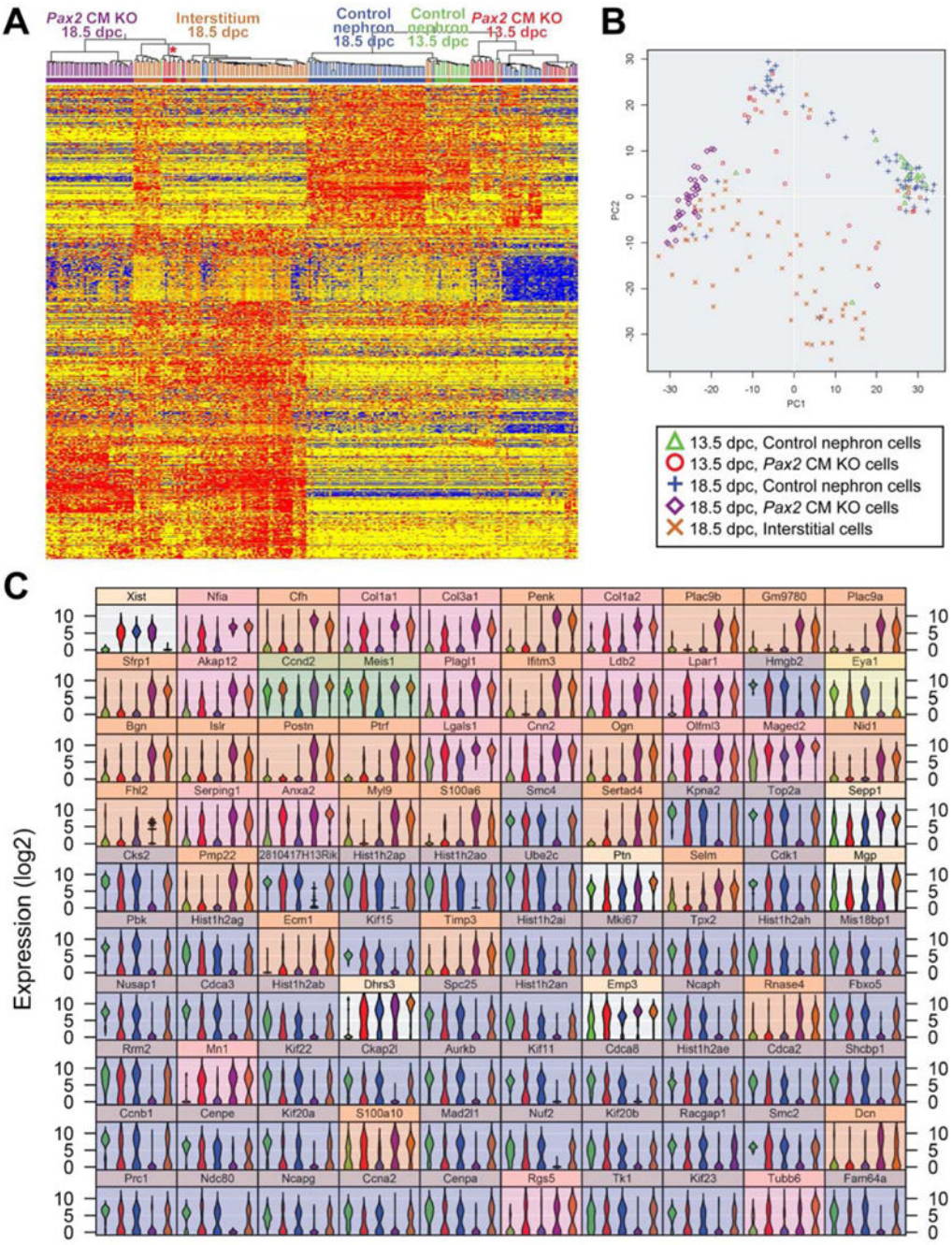

Figure 7. Gene expression profiles for *Pax2*-mutant cap mesenchyme-derived cells are similar to those in renal interstitial cells than nephron epithelial cells, but distinct

(A) Heat map and unsupervised hierarchical clustering by GeneSpring for single cell RNA-seq analysis of *Pax2*-mutant cap mesenchyme-derived cells in *Six2-eGFPCre*$^{tg/+}$; *Pax2*$^{flox/del}$; *R26R-CAGGS*$^{tdTomato/+}$ mutant kidneys at 13.5 and 18.5 dpc, control nephron cells from *Six2-eGFPCre*$^{tg/+}$; *Pax2*$^{flox/+}$; *R26R-CAGGS*$^{tdTomato/+}$ kidneys at 13.5 and 18.5 dpc and renal interstitial cells from *Foxd1*$^{eGFPCreERT2/+}$; *Pax2*$^{flox/+}$; *R26R-CAGGS*$^{tdTomato/+}$ kidneys at 18.5 dpc following 2 mg tamoxifen injection at 11.5 dpc. The red asterisk

indicates *Pax2* mutant cells expressing interstitial genes at 13.5 dpc. (B) PCA plot by AltAnalyze. (C) Violin plot for the top 100 discriminating genes by AltAnalyze.